QATAR UNIVERSITY

COLLEGE OF ENGINEERING

TREATMENT OF PRODUCED WATER USING AN ENHANCED ELECTROCOAGULATION PROCESS

BY

MUSTAFA MOHAMAD AL-GHOUL

A Thesis Submitted to the Faculty of

the College of Engineering

in Partial Fulfillment

of the Requirements

for the Degree of

Masters of Science in Environmental Engineering

June, 2017

COMMITTEE PAGE

The members of the Committee approve the Thesis of Mustafa Al-Ghoul
defended on 21st of May, 2017

Dr. Alaa Al hawari
Thesis/Dissertation Supervisor

Dr. Ramazan Kahraman
Committee Member

Dr. Md Monwar Hossain
Committee Member

Approved:

Khalifa Al-Khalifa, Dean, College of Engineering

ABSTRACT

Al-GHOUL, MUSTAFA, Masters of Engineering: June, 2017, Masters / Environmental Engineering

Title: Treatment of produced water using an enhanced electrocoagulation process

Supervisor of Thesis: A.Al Haawari

Produced water generated during oilfield processes is considered as a major problem that requires solving due to its high salinity and pollutant contents. Electrocoagulation is one of the promising processes for produced water treatment. In this study, steel slag was used as an additional coagulant in the electrocoagulation process for the produced water treatment. The impact of current density, reaction time and the amount of added steel slag were investigated. For a current density of 10 mA/cm^2 at a 10 minute reaction time, it was found that the slag sample had a total suspended solids removal of 90% compared to 55.7% for the pure sample. As for the turbidity the slag sample showed an 85.9% removal, and the pure sample showed an 80.1% removal. The oil and grease removal percentage were almost the same for the sample with and without the slag at 98.9% removal. For the reaction time, it was found that as the reaction time increases the percentage removal for the total suspended solids and turbidity increases to a certain extent. The optimum removal percentage was obtained at a reaction time of 30 minutes. It was found that the slag sample had a 94.8% and a 92.5% total suspended solids and turbidity removal percentages, respectively, while the pure sample had a lower removal percentage of 90% and 90.3%, respectively. The oil and grease removal percentage were similar for both samples where it was 98.6% for the slag sample, and 98.9% for the pure

sample. The impact of the amount of added slag was studied for 3 different concentration : 5g/L, 10g/L, and 15g/L. It was found that the optimum removal percentage of suspended solids, turbidity, and oil and grease were 83%, 55%, 96.5%, respectively, using a slag weight of 5 grams.

DEDICATION

This work is dedicated to my parents and friends, who without their support and continuous help, none of this would've been possible.

Thank you all for your help.

ACKNOWLEDGMENTS

I would like to take the chance to thank Dr.Alaa al hawari for his great help and support through the research period. His continuous encouragement, innovation and critical thinking, is what helped us through the difficult phases of the research. He has been nothing but an amazing mentor to me, whom I shall follow his steps.

Special Thanks goes also to Mr. Gad and to Mr. Al-Jamal, who provided me with an enormous amount of help from day one and until this day, in terms of providing various technical expertise that contributed greatly in my research.

Thanks to the civil engineering department in Qatar University, for providing a safe and a professional working environment to conduct our research in.

TABLE OF CONTENTS

LIST OF FIGURES

LIST OF TABLES

Chapter 1 LITERATURE REVIEW

1.1. Produced water in Qatar

Qatar is considered as one of the major gas producers around the world producing over 77 MTA of LNG as well as other petrochemical products such as GTL. In the oil and gas production process a huge amount of produced water is generated with an estimated 4 barrels of produced water for each oil barrel produced.(Adham, 2015)

According to Qatar Petroleum, Qatar produces over 88.7 Million barrel of oil per year throughout its varied drilling sites such as the north field, the offshore fields such as Maydan Mahzam, and the onshore field such as Dukan Field. The production capacity of all these fields combined of produced water is estimated by a 345 Million barrel per year of produced water. The quality of this water varies depending on the origin of the water, whether it was originally in the well, or whether if the water was injected into the well to enhance the oil and gas recovery process.(Petroleum, 2015)

Figure 1: Typical oil and gas reservoir (Norman, 2017)

Produced water has many pollutants that require treating such the turbidity, the salinity, COD, and the heavy metals content. In order to meet with the regulatory demands, many plants and organizations nowadays are implementing techniques to reuse, recycle, and manage the produced water production process. These techniques can be as follows:

1- Avoiding produced water production on the surface: This is achieved by injecting a polymer gel which blocks water from reaching the surface, or by installing water separators, that separate water from oil and gas and re-inject water in any suitable formations.
2- Produced water injection: This is achieved either by injecting the produced water in the same formation from which it was taken from, or into a similar formation. Treatment process are sometime implemented to get rid of any fouling, scale or bacteria from the water prior it's injection.
3- Produced water Discharge: This is achieved by discharging the produced water after its treatment and ensuring that the quality of the water produced is meeting local and international regulations.
4- Produced water usage in oil operations: Produced water is used after it's treatment to meet operation quality in drilling and other oil and gas extraction related process.
5- Produced water treatment for other usage: This is done, by treating produced water to meet local regulations from the water to be used in irrigation and other usage such as district cooling. Water treatment process are as a result are

implemented to ensure a safe reuse, recycle and disposal of the produced water is achieved.(Arthur et al., 2005).

The characteristics of produced water varies based on its geological location. As per the U.S. Geological Survey National Produced Waters database, the characteristics of the water can be seen in Table 1 and Table 2

Table 1*:*

Inorganic constituent in conventional produced water(Blondes et al., 2016)

Constituent	**Concentration Range (ppm)**	
	Low	High
TDS	100	400,000
Sodium	150,000	150,000
Chloride	250,000	250,000
Barium	850	850
Strontium	6,250	6,250
Sulfate	15,000	15,000
Bicarbonate	15,000	15,000
Calcium	74,000	74,000

Table 2*: :*

Organic constituent in conventional produced water (Blondes et al., 2016)

Constituent	Concentration Range (ppm)	
	Low	High
TOC	*ND	1700
COD	1220	
TSS	1.2	1,000
Total Oil	2	565
Volatiles	0.39	35
Total Polars	9.7	600
Phenols	0.009	23
Volatile Fatty Acids	2	4,900

***ND = Below Detection Limit**

1.2. Produced water treatment

The high demand on fresh water resources created the need to find and utilize technology to treat the produced water, the quality of the produced water from any application varies from one another. The direct usage of produced water is considered as a biological hazard, which might cause harm to the environment. Hence the development of the

treatment methods and their application to produced water is very important in order to recycle and reuse them. The purpose of produced water treatment is the removal of any pollutant that may have an adverse effect on the environment. Pollutant such as organic matter that consumes oxygen from water, chemical nutrient such as phosphorous and nitrogen, bacteria, metals, odors, and suspended solids that exits in the production.

Furthermore, removal of such pollutants is carried out over several stages with specified process (Chin, 2006):

- Chemical Process: where chemicals are used to separate dissolved and suspended particle. These particles tend to not be removed using physical process and hence requires the addition of certain chemicals to be separated. However, the addition of these chemicals tends to have a negative side on the treatment process considering the additional costs. An example of this chemical process can be flocculation and coagulation.
- Biological Process: Where bio degradable material is removed by the addition bacteria that removes any and consume any organic content as well as any nutrients. When process is carried in the presence of oxygen, they are referred to as aerobic, while in the depravity of oxygen their called anaerobic. An example of that can be the activated sludge process.
- Physical Process: Where solid and biomass are removed by physical process without the addition of any chemicals or any bacteria. Examples of that can be filtration and sedimentation tanks.

Table *3:*

Produce water treatment unit operation (Chin, 2006)

Unit Operation	
Physical Process	Flotation
	Sedimentation
	Filtration
Biological Process	Anaerobic Process
	Aerobic Process
Chemical Process	Adsorption
	Membrane Separation
	Chemical Oxidation
	Coagulation/ Electrocoagulation

1.2.1. Oil and grease treatment in produced water

Oil and grease removal from produced water means the removal of oil in all of its forms from the produced water. These forms can be as normal oil (Free), dispersed and emulsified oil droplet. The treatment process of the oil and grease should meet the USEPA standards, for it to be used again oil and gas drilling services. The USEPA limits for a maximum limit for O&G of 42 mg/L per day and a 29 mg/L per month on average.

Moreover, the following technologies are commonly used to treat the oil and grease based on their different particle size.

Table 4*:*

Oil and grease removal technologies based on oil and grease particle sizes (Arthur et al., *2005)*

Oil Removal Technology	**Minimum size of particles removed (microns)**
API gravity separator	150
Corrugated plate separator	40
Induced gas floatation (no flocculants)	25
Induced gas floatation (with flocculants)	3 – 5
Hydrocyclone	10 – 15
Mesh coalescer	5
Media filter	5
Centrifuge	2
Membrane filter	0.01

API separator and hyrocyclone are the two most common technologies used to treat the produced water for variable aspects. API gravity separator is based on gravity where the particles are left to settle down under the force of gravity only, where these the oil particles tends to flocculate or coagulates under the right operating conditions. This lead to the fact that the separation process is dependent on the retention time and the design of the tank. However, as the oil particles properties vary, the efficiency of the separation process tends to change, especially when considering smaller or emulsified oil droplets. Another side effect for this process is that it requires a high capital cost, long maintenance time as well as the quality of the treatment of the produced water being dependent on the design of the tank.(Pintor et al., 2016)

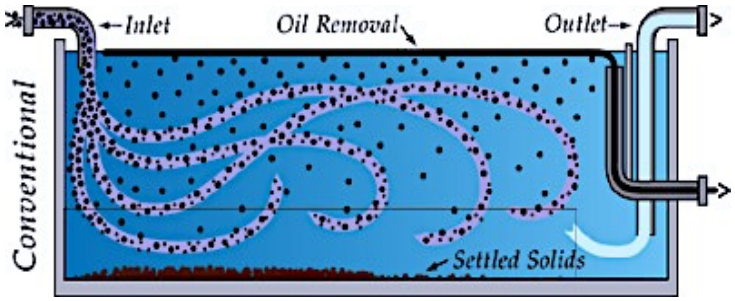

Figure 2: Typical separator (Systems, 2014)

Hydrocyclones is another piece of technology that utilizes the centrifugal force to separate heavy water particles out, while keeps the light oil droplet in the middle of the cone. The addition of gravity provides a better separation process. The technology of such device provides a better removal even at high oil organic concentrations. A side effect that takes place in this process at normal operating conditions is the large pressure

drop within the device causing a limitation in the removal process of any other solids as well as the high maintenance costs , and the blockages by solids accumulation within the bottom of the cone or on its surface.(Mines, 2009)

1.2.2. Soluble organics treatment in produced water

Water soluble organics are organics present in the water of the produced water. It is considered as a part of the oil and grease within the produced water, but can't be removed with the conventional methods used to treat oil and grease. This is due to its solubility in water. Some compounds are partially formed in small quantities are aromatics such as benzene, toluene, ethylbenzene, and xylenes. These compounds tend not to be effected by pH greatly. However, some of the polar hydrocarbons such as the fatty acid are sensitive to the pH and tend to change their solubility in water based on it. At a high pH these fatty acid will be in ionic form and will tend to be soluble in water. At a low pH they will tend to form carboxylic acid molecules which aren't as soluble in water. This is shown in Figure 3

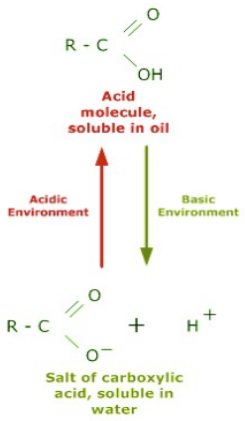

Figure 3: Fatty acid changes within different pH mediums (Keeper, 2013)

A common method used to treat water soluble organics is by adsorption. Adsorption columns filled with adsorbent solids that are stacked in pours increase their surface are with the produced water to be treated. The higher the pours and the surface area of the column, the higher the removal percentage of these organics. Adsorbent can extend to a wide range of filtrate such as activated carbon and clay. A key factor that limits the effectiveness of the process is the retention time and the capacity of the column. Another approach used to treat water soluble organics is by oxidation by strong oxidizer such as H_2O_2, O_3 , or OH ions. These oxides tend to dissolve any organics into CO_2, which is then stripped by UV air stripper.

1.2.3. Total dissolved solids treatment in produced water

Dissolved solids and salts is another pollutant needed to be removed from produced water (i.e.: TDS in produced water is estimated by an average of 2,000-150,000 ppm). The selection of the desalination technology is greatly dependent on the quality of the produced water and the TDS concentrations. Technologies such as membrane, evaporation and filtration and electrocoagulation are the common methods to treat dissolved solids.

1.2.4. Advanced treatment of produced water

The produce water contains various amounts of algae and bacteria to be treated in ordered to prevent scale formation or any contaminant in the water after it's treatment. Treatment technique of such contaminants include the use of various chemicals such as chorine, O_3 or the use of pH variation chemicals. An alternative treatment method include the use of UV light.(Keeper, 2013)

Several researches are being conducted to evaluate the efficiency of each of these technologies as well as the feasibility of their applications in real work environment. (Xu et al., 2011) .One technology that hold high potential in terms of cost effectiveness and maintenance cost as well as oil and grease removal percentage is the electrocoagulation process.

1.3. Electrocoagulation treatment process

1.3.1. Electrocoagulation

Electrocoagulation process, discovered by Michael Faraday in the 19th century, utilizes the electrochemistry science to coagulate, flocculate and oxidize particles in waste water. (Chen et al., 2005). In electrocoagulation an electric current passes through an electrolyte between two electrodes resulting in a chemical reaction (Lin et al, 1998). The electrocoagulation process is able to remove pollutants from water by electro flocculation, electro coagulation and electro oxidation, where these pollutants are removed by destabilizing and neutralization of the repulsive forces between the suspended particles. These forces, once neutralized, will cause the suspended particles to form larger particles, and hence settle down. This allows an advantage for this process over other processes and that is the ability to treat oily water. This happens as a result of the electric current taking part in the electro coalescence of oil droplets that are considered quiet small (Mhatre et al., 2015).

1.3.2. Colloidal particles stability and destabilization

Electrocoagulation process is considered as an efficient process that utilizes its ability to destabilize any oil emulsion when in water. This takes place as a result of the oil droplets having a negative net charge at their surface. According to Helmholtz theory, an electrical double layer is formed between the negative oil droplet and the positive ions from the surrounding solution bulk layer. (Volkov et al., 1996). This double layer potentials' tends to decrease when moving away from the oil droplet surface, creating a

repulsive force between oil droplets surfaces and hence preventing them from colliding. This force is represented by zeta potential which is the potential difference between the surface of the droplet surface and the surrounding bulk. It helps in identifying whether or not emulsion will stabilize or not within the solution, where the higher its value the higher the chances for the emulsion to stabilize during the electrocoagulation process (Volkov et al., 1996). The electrical double layer and its regions can be illustrated in Figure 4.

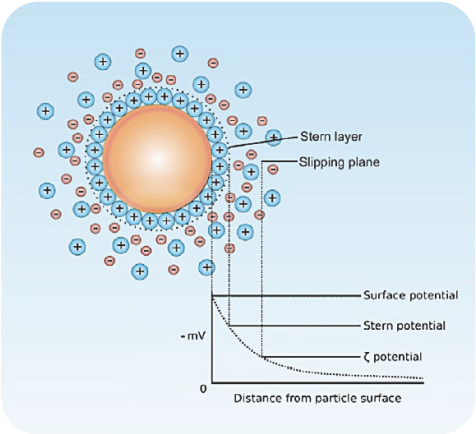

Figure 4: Double layer electrical potential regions form around an oil droplet (Volkov et al., 1996)

Breaking these emulsions in the bulk solution can be contributed to two processes. The first process takes place when the ions generated at the anode start neutralizing the charge of the ionic species present in the water resulting in reducing the electrostatic antiparticle repulsion between the oil droplet and the bulk water, which in return forms flocs that settles down in the form of sludge (Mollah et al., 2004). The

second process takes place as a result of a reaction at the cathode, where hydrogen bubbles are formed resulting in an adhesion between the oil droplets and the hydrogen bubble, which in turn rise to the surface in the form of sweep flocculation. (Bennett et al. , 1988).

1.4. Steel slag

Steel slag is a by-product produced in modern days' steel manufacturing process. It is produced during the steel separation process from impurities taking the form of a molten liquid metals, which once solidified, turns into metal oxides and silicates solids. The steel slag consists primary from Fe_2O_3, CaO, and some other metals such as Mn, Mg and silicate materials.

In general, the steel is produced via two technologies now days, the oxygen steel convertor and the electric arc blast process. In the oxygen steel convertor process, steel is manufactured by different stages starting with the blast furnace where the steel is separated from other inlet components and impurities such as slag. After that the steel is produced to transferred from the bottom of the furnace to a transportation ladle, where a layer of slag is formed on top of it called Ladle Slag. After that the product is taken in the oxygen convertor where any impurities such as calcium and silicate are oxidized under the effect of excess oxidization process, resulting in the formation of slag as by-product called raker slag. Followed by that, the steel is introduced to the ladle, where extra impurities are removed from the steel exiting the oxygen converter, by introducing an inert gas to the mixture, resulting in the formation of the slag on the surface of the ladle

referred to as the pit slag, which is then removed. The slag process throughout the process would have different characteristics and qualities ranging from high to low depending on its disposal location. Figure 5 shows the disposal location, in which the slag is produced throughout the steel manufacturing process in order from top to bottom.

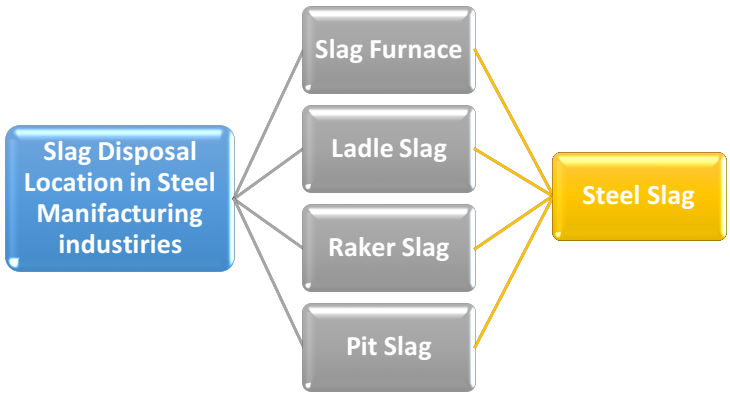

Figure 5: Steel slag disposal location in steel manufacturing industries

Qatar steel produces an estimate of 400,000 tons of slag every year. The production of such amount poses a difficult problem to solve in terms of disposal or recyclability for the company and for Qatar in general. One of the solutions the poses potential for the slag usage is its usage in the electrocoagulation process of produced water.

1.5. Previous electrocoagulation studies on produced water

Several recent papers studied variable aspects of the oil and grease as well as the suspended solid and other pollutant removal from the water samples using various configurations and operating condition of the electrocoagulation process recently

Rupesh, reported using the electrocoagulation process to treat oil field produced water from emulation oils particles. In his experiment, perforated aluminum electrodes were used under different reaction times, voltage and pH. The effect of the running voltage and the running time on the oil and grease removal percentage and the relation of the NaCl percent in the sample were studied in the experiments as well. His findings showed 90% oil and grease removal efficiency under these conditions at a 20 minutes' runtime and 5V at a 4.72 A current. (Bande et al., 2008).

Kirt also achieved similar removal percentage, when treating biodiesel waste water from oil and grease using iron electrodes, reaching the optimum conditions at a18.2 V, 23.5 minute of reaction time and a pH of 6. The initial oil and grease concentration was at 18000-22000 ppm and was decrease to 80 ppm when at 25 minute reaction time and at a current density of 100 A/m^2(Ngamlerdpokin et al., 2011).

Moreover, Xinhua in his treatment of oily refractory water, considered many factors and operational parameters, such as the current density, the conductivity, the electrode distances as well as the initial pH of the water prior the electrocoagulation treatment. By trial and error, the optimum operating conditions were found to be at a current density of 10-14 A/m^2 at 30 minute of reaction time, with no effect of the

conductivity on the generated results what so ever. The final oil and grease removal efficiency achieved was estimate at 90% removal percentage (Xu and Zhu, 2004).

Additionally, In 2008 Guillermo studied the removal of oil and grease as well as other heavy metal such as Cu, and Ni from a sample of synthetic bilge water. The electrocoagulation process was carried out in a continuous flow reactor. The continuous reactor was run at volumetric flow rate of 1L/min, and the electrodes used were made of carbon steel and as well aluminum, at a current density of 0.6 A/m^2. The electrocoagulation process showed high oil and grease and heavy metal removal percentage, with an estimated 99% removal for the oil and grease decreasing from 5000 ppm to 10 ppm at the mentioned conditions(Rincón et al., 2014).

According to Merma who studied the Electrocoagulation process of oily water in general to identify the key factors that affect the amount of sludge generated and the pollutants removed from the treated waste water. Synthesized oil water was obtained from shell by him of an oil concentration of 3000 ppm and variable operating conditions of the electrocoagulation process in terms of electrode configurations and material were studied .The results showed that the hydrogen bubbles generated at the cathode and hence the amount of flocculants and sludge generated in the solution and the pollutants removed, greatly depends on the material of the electrodes used, the pH of the solution as well the surface area of the electrode exposed to the surrounding solution (Merma & Leonardo, 2008).

The results generate and much more show high potential for oil and grease, turbidity and the TSS removal from produced water using the electrocoagulation. The

efficiency and the removal percentage of each one of these parameters, is determined by several factors such as the current density, the reaction time, the frequency of the reaction timing, the initial pH and conductivity of the solution, as well as the material of the electrodes used and the distance between them. In this project, only two parameters were studied extensively and they are the current density and the reaction time

The current density holds a great important for the electrocoagulation process. The amount of sludge, bubble formation as well as separation process of the pollutants from the waste water, is greatly dependent on the amount of current density supplied throughout the system. The greater the current density, the higher the removal percentage of any pollutants such as the turbidity, the total suspended solids as well the oil and grease(Nanseu-Njiki et al., 2009).

De-colorization is another aspect that is dependent on the current density used and the material of the electrodes used, where the de-colorization effect can reach up to a 90% removal efficiency (Daneshvar et al., 2004).

Moreover, according to Tir, the increase in the current density increase the amount of $Fe(OH)_3$ generated in the solution, which enhances the coagulation and the destabilization process (Tir & Mostefa, 2008).

However, the excess generation of the hydrogen at the cathode resulted from increasing the current density can result sometime in an adverse effect on the coagulation process if not controlled properly as reported by Guohua. (Chen, 2004).

The size of the hydrogen bubble greatly effects and can hinder the effectiveness of the current density from forming any colloids, and hence the removal efficiency as reported

by chen et al. (2002). Furthermore, the excess increase in the current density can hold other side effects on the separation process. Effects such as the high operating cost in terms of power consumption, as well as an excess usage of the electrodes and their consumption.

The reaction time of the electrocoagulation process, is another important factor to be considered in that would greatly influence the coagulation process. At longer reaction time the amount of coagulants generated in the solution from the electrodes greatly increases, which in turns increase the removal efficiency of all the pollutants present. This takes place as a result of the metal hydroxide generated from the anodes, will tend to destabilize the oil and grease collides and particles and coagulate them at a longer reaction time causing them to destabilize as reported by Chou(Chou et al., 2009). Although removal efficiency at longer reaction times can up to 99% percent from the oil and grease removal at a longer reaction times. However, this would cause adverse effect on the treatment process, because of the increase in the power consumption due to the longer reaction times, as well as extra cost for the electrodes and their reusability, and the materials used to clean the electrodes. This can be avoided by finding the optimum reaction time, at which high efficiency is achieved, without the need for longer reaction time to minimize the cost.

The purpose of this research is to use steel slag as a potential additive in order to enhance the electrocoagulation process. The impact of different parameters will be studied:

1) The reaction time (i.e. 10, 30, and 60 minutes).
2) The current density (i.e. 10, 30, and 60 mA/cm^2).
3) The amount of added steel slag per liter of produced water sample (i.e. 5, 10, and 15 g).

Chapter 2 EXPERIMENTAL METHODS AND PROCEDURE

2.1. Experimental setup

The EC treatment process was run in a 1-liter volume beaker containing produced water with two rectangular aluminum plates (9.8 cm x 5.5 cm) of 1 mm thickness and a gap distance of 2.5 cm, were submerged in the water and were connected to a DC amplifier. Figure 6 shows a view of a two aluminum plates mounted on a poly vinyl chloride spacer of 2.5 cm.

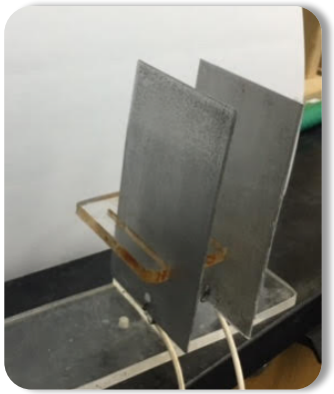

*Figure 6:*The mount holding the Anode and the cathode with a 2.5 cm spacing

Prior using these aluminum plates, they were cleaned from any metal oxidants using hydrochloric acid and sand paper. The aluminum plate connected to the positive amplified input served as an anode, while the one connected to the negative input served as a cathode. The amplifier allows in changing the current and voltage supplied to the system and hence, changing the current density supplied through the anode over any period. The beaker on the thermal plate was to allow the magnetic stirrer within the beaker to provide a uniform mixing of the generated chemicals within the produced water, when the electrochemical reaction takes place. An overall view of the setup is seen in Figure 7. The experimental set up was divided into experiment to be run at the same time. One sample contained a pure produced water sample, while the other contained varied amount of slag. Figure 8 shows an overall view of the EC system used in the produced water treatment, with the left sample containing pure produced water while the left sample contain 5 grams of slag.

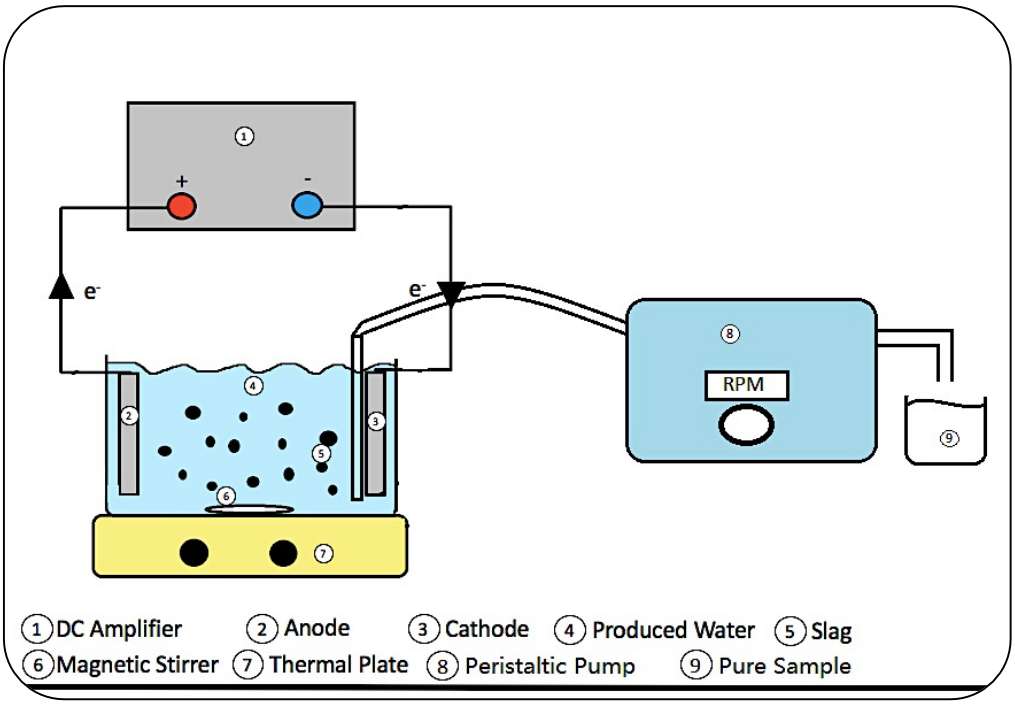

Figure 7: Schematic Diagram of the EC system

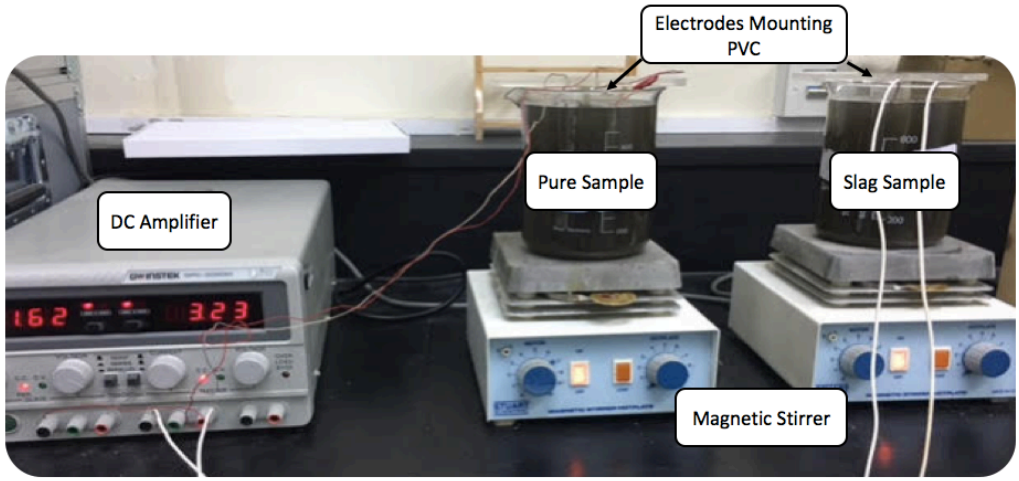

Figure 8: Overall view of the EC system used , with a slag containing run and a pure sample run.

The experiments conducted were carried out over 250 RPM stirring, at a temperature of 22.5^{o}C, over different timelines of 10, 30, and 60 minutes, and different current densities of 10, 30, and 60 mA/cm^{2}. After the experiments, the amplifier was switched off, and the stirring stopped, where the sample was left to settle down for 2 hours. After that time the a sludge layer was formed at the bottoms of the beaker, while a flocculent layer is formed on its surface. A tube is inserted into the sample prior to its settling, to allow the sample collection process without causing any disturbances in the sludge and the fluctuant layers, where a peristaltic pump was connected to this tube and a 150 ml sample was taken for the oil and grease, TSS and turbidity analysis. The aluminum anode used in the process weight is measured before and after the process for the anode reduction percentage, and the rest of the produced water formed from the reaction is taken for sludge analysis using the imhoeff cone.

2.2. Experimental analysis

2.2.1. Conductivity and pH measurement

The conductivity of the produced water and its pH is carried out before and after the electrocoagulation process, to ensure that the decrease in the produce water temperature, will not affect the pH and the conductivity. This was achieved by collecting a small sample from the treated water and getting the required reading of it. It's worth mentioning that the conductivity of the produced water was considered high salinity, while maintaining a neutral pH at 6.2 pre-treatment.

2.2.2. Total suspended solids measurement

The total suspended solids removal was measured for the sample in hand, pre-and after treatment in order to estimate the percentage of removal, and hence to evaluate the effectiveness of the slag on the treatment process over the non-slag containing sample. A sample of 150 mL was collected from the pure treated sample and the slag containing sample after 2 hours of settling time. These samples can be seen in Figure 9. Out of the 150 mL samples, 50 mL were used for the TSS measurements, and a 100 ml were used for the oil and grease measurement.

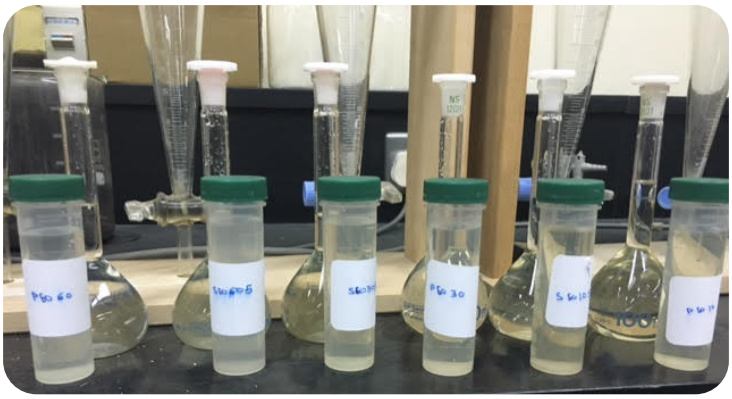

Figure 9: 50 mL samples used for TSS measurements alongside 100 mL samples used in the oil and grease measurement

The samples collected where filtered using TSS Glass Fiber Filter of Pore Size 1.5 µm and a suction pump. Initial weight reading were recorded, and then the filtrate was placed in an oven at 105 ^{O}C for 2 hours' period to remove any organic material and any liquid

traces from the filtrate. After that, the sample were left to cool down, and were weighted again for the TSS calculation. The TSS samples after being dried of are seen in Figure 10.

Figure 10: TSS papers sample after being heated over 2 hours at 105 ºC

The equations below were used to calculate the TSS:

$$TSS\ (ppm) = \frac{Paper\ Weight\ After(grams) - Standard\ Paper\ weight(grams) x\ \frac{1000mg}{g}\ x \frac{1000mL}{L}}{50\ mL}$$

After calculating that the percentage of TSS removal was calculated by comparing the sample TSS with the raw produced water sample's TSS weight according the following equation:

$$Percentage\ of\ removal = \frac{Raw\ produced\ water\ sample\ TSS - Treated\ sample\ TSS}{Ra\ w\ produced\ water\ sample\ TSS}\ x\ 100\%$$

2.2.3. Turbidity measurement

The turbidity of the produced water was measured pre-and after EC treatment process. Samples of 25ml were taking in the same manner as the TSS sample to ensure a clear solution as possible. These sample were then measured for turbidity using Hach 2100P. Prior the measurement of any samples, the device was calibrated and the glass container samples were cleaned with water and soup to ensure that the remaining of any previous samples were removed, after which, the sample were measured.

2.2.4. Oil and grease measurement

Oil and grease concentration were measured as well for all samples using the ASTM D 7066-04 standards. The technique used in doing so was liquid separation carried out on different stages. To measure oil and grease concentrations at first 100 ml of the sample was taken and mixed with a 20 ml of S316 polymeric solvent and a 1 ml of 1:1 HCl. This mixture was then well mixed for 5 minutes in a conical flask, and left to separate for 10 minutes. Figure 11 shows the liquid separation process for a slag containing sample and a pure one.

Figure 11: Oil and grease liquid separation process

When the separation was noticed after 10 minutes, the bottoms layer (the Oil layer) was let to run through a filter paper containing sodium sulfate to prevent any liquid from reaching the collected sample. The sample collected was then measured on Horiba oil content analyzer OCMA 350.The reading given by the device were interpolated into the actual reading in ppm as the follows

$$Oil\ and\ Grease\ Concentration\ (ppm) = \frac{Reading(ppm)\ x\ Dillution\ Factor\ x\ Extraction\ Vol.(mL)}{Sample\ Vol.(mL)}$$

2.2.5. Sludge measurement

Sludge measurement was preceded after the EC treatment process. After all the reading were recorded for the rest of the tests, the left of the sample was spilled into several graduated imhoef cones the solutions were left to settle down over night and then the readings were obtained. Readings obtained from the measurement were conveyed by ml of sludge per Liter of total solution volume. Figure 12 Shows the sludge formation in a slag containing sample and in a pure one.

Figure 12: Sludge volume reading through imhoef cone for a slag containing sample (left) and pure sample (right)

2.2.6. Anode consumption

Aluminum plate weight reduction or gain were measured for all aluminum plates, both before and after EC treatment process. Prior the usage of the aluminum plates, they were cleaned with hydrochloric acid, to ensure that there isn't any metal oxide on the surface of the aluminum plate that would hinder the electrocoagulation process. After that

the plates initial weights were recorded. After the EC treatment process, the aluminum plates were washed with water thoroughly, and measured again to be compared to their original weight. Anode reduction or consumption percentage was measured by comparing the pervious anode weight to the weight after the process and dividing the difference over the original anode weight. Figure 13 shows 4 aluminum plates, 2 anodes and 2 cathodes after being cleaned for measurement after the EC treatment process.

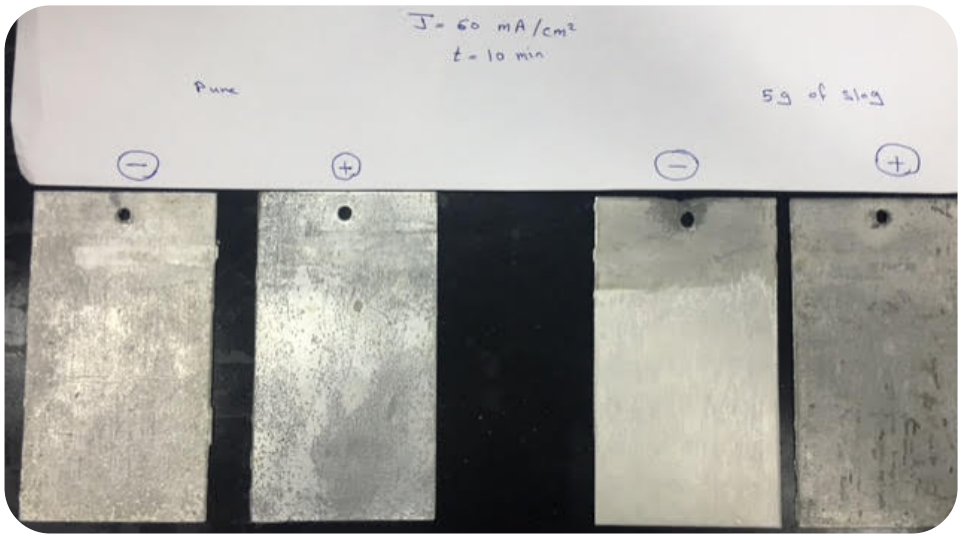

Figure 13: Aluminum plates weight measurements after ec treatment

2.3. Produced water characterization

The produced water used in the experiment was synthesized in the lab. The characteristics of the water is as in Table 5.

Table 5*:*

Synthesized produced water characteristic

pH	6.3
Conductivity (mS/cm)	94.4
Oil and Grease (ppm)	950
Total Suspended Solids (ppm)	3116
Color	Black
Turbidity (NTU)	915
FeSO4 (ppm)	100
CaCl2 (ppm)	7000
KCl (ppm)	2000
MgCl2 (ppm)	7500
NaCl (ppm)	55000
Na2SO4 (ppm)	2000
NaH2PO4 (ppm)	40
NaHCO3 (ppm)	1000
H3BO3 (ppm)	200

2.4. Slag characterization

The used in these experiments were extracted from a steel producing plant in the state of Qatar. This steel slag sample used was mainly formed from ferric oxide and calcium oxide at a 40% of the total weight, and 20% of other metals such as Mg and Al. The particles of steel slag tend to have a gravel like textures, while having a blackish particles color accompanied by the presence of a white dust particles trapped within these slag particles. Prior using these slag sample in the process, they were first cleaned and washed with water multiple times, and dried in the oven over night. This was done to ensure that they are no dust particles trapped within the slag particles so as not to affect the EC process. After that the slag sample was grinded to a 425-nm particle size, allowing the particles to have highest/largest surface area, ensuring and providing high efficiency and performance to the reaction taking place in the electrocoagulation process. Figure 14 shows several slag samples, each grinded at a different particle size.

Figure 14: Steel slag sample grinded to a different particle size.

2.4.1. Scanning electron microscope

SEM short for scanning electron microscope is a technology that emits high energy electrons on the surface of a sample to generate a high-resolution image of the sample grains, size, crystalline structure, texture and orientations, covering areas ranging from 1 cm to 5 microns in width.(Argast & F. Tennis III, 2007) . The SEM analysis was conducted on the slag sample both before and after the EC treatment process as will be seen in the results and discussion section later.

2.4.2. FTIR analysis

FTIR short for Fourier Transform infrared spectroscopy is a technology that utilizes the infrared spectrum of absorption, emission and the Raman scattering of any material. This is achieved by collecting a wide range of spectral data achieved by measuring the intensity of the dispersive infrared over certain ranges of wavelength. This allows for the detection of certain functional groups within the sample. Moreover, The FTIR was used to identify organic functional groups within the slag added to the sample, both before and after the electrocoagulation process, to give an indication of whether any new groups are formed or added to the slag after the electrochemical treatment of the produced water sample.

2.4.3. Energy dispersive X-ray analysis

Energy Dispersive X-ray analysis (EDAX) is one type of the spectral analysis that is used to identify and characterize chemical components and their elements. The way an EDAX works is by emitting an X-ray beam into the sample, which once reaching the

surface of the sample, electrons at higher valence levees are excited and hence jumps out of the sample to a detector. This emitted X-ray from the sample tend to have a certain wavelength, which depending on the sample's elements, will have a different X-ray wavelength, allowing the device to identify the elements and its atomic weight percentages. This method was used to identify the differences between two slag samples, One of which prior EC treatment process, and the other after the process.

Chapter 3 RESULTS AND DISCUSSION

The Performance of the pure sample and the slag containing sample were studied separately, for the total suspended solids, the turbidity and the oil and grease removal, considering certain parameters such as the effect of the current density supplied during the electrocoagulation process and the reaction time. After which, both samples performances were compared to each other to study the effect of the slag addition and the effect of its weight added to the pure sample's TSS, turbidity and oil and grease removal percentage against the current density and the reaction time.

3.1. The performance of the pure sample

The total suspended solids, turbidity and oil and grease removal percentage is studied, for 6 pure samples, 3 of which are studied with variations in the current density ranging between 10, 30, and 60 mA/cm^2, while at different timelines, and the rest are studied by setting periods of reaction time ranging between 10,30, and 60 minutes, while at different current densities.

As the EC process tool place, several reactions took place in the system, but most importantly was the dissolution of the metallic anode cations and the generation of the hydroxyl ions and the hydrogen gas at the cathode. The system used in the case of this experiment used aluminum metal as a cathode and anode for the electrocoagulation process over the widely-used steel anodes. This is due to the fact that the aluminum electrodes show a better removal percentage in terms of total suspended solids, turbidity and discoloration over the steel electrodes, even though their price is a bit higher (Demirci et al. , 2015). Merzouk et al. (2009) and Thella et al. (2008) stated that the following reactions took place, when two aluminum electrodes are used in the electrocoagulation process.(Thella et al., 2008) (Merzouk et al.,2009)

The anode reactions:

$$Al \rightarrow Al^{+3}_{(aq)} + 3e^{-}$$

$$Al \rightarrow Al^{+2}_{(aq)} + 2e^{-}$$

The aluminum will tend to dissociate and oxidize into aluminum (II) and (III) ions from the surface of the anode into the water, resulting in generating electrons that pass through the external circuit into the cathode. The generation of the Al^{+3} will stabilize colloidal particles by stabilizing their charges. Moreover, another reaction will tend to take place at the anode as well, due to the high salinity of the produced water used in the experiment, resulting the in the following reaction below, from which more electrons are going to be generated in the external circuit, while more O_2 and $H_{2(aq)}$ are generated within the water.

$$2H_2O_{(l)} \rightarrow 4H_{(aq)}{}^{+} + O_2 + 4e^{-}$$

$$2Cl^- \rightarrow Cl_2 + 2e$$

At cathode, the water will react with the surface of the cathode and the following reactions take place:

The cathode reactions

$$2H_2O_{(l)} + 2e^- \rightarrow H_{2(g)} + 2OH^-$$

$$2H^+ + 2e^- \rightarrow H_{2(g)}$$

The overall reaction is as follows:

$$Al^{+3} + OH^{-1} \rightarrow Al_2(OH)_3 + H_{2(g)}$$

It's worth mentioning that some aluminum ions at the anode will be in hydroxide form, forming a wide range of unstable aluminum hydroxides, that are stabilized by the produced water content, by the hydroxides generated at the cathode, or by the chloride generated at the anode.

3.1.1. Effect of current density

The Total suspended solids, turbidity and oil and grease removal percentage were studied, for 3 pure samples, each of which was set at a current density ranging between 10, 30, and 60 mA/cm^2, for a period of time between 10 to 60 minutes. This is achieved to assess the effectiveness of current density variation on the parameters' percentage of removal. The samples with different current densities are given abbreviations as follows: CD10- sample with a current density of 10 mA/cm^2, CD30- sample with a current density of 30 mA/cm^2 ,and CD60- sample with a current density of 60 mA/cm^2 .

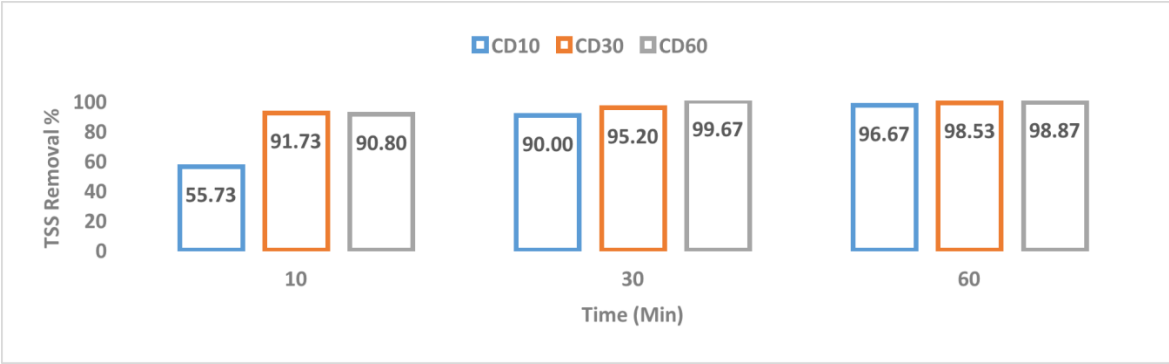

Figure 15: TSS removal for 3 pure samples at different current densities at different timelines

Figure 15 shows the total suspended solids removal percentage in 3 pure samples, each run at a three time intervals ranging between 10, 30, and 60 minutes at different current densities of 10, 30 and 60 mA/cm^2. At 10 minutes' reaction rime, CD10 sample showed the lowest TSS removal with 55.73% removal, while the CD30 sample is showed the highest removal at 91.73%. As for the CD60 sample the removal percentage was 90.8%. As the reaction time reaches 30 minutes, the TSS removal percentage was enhanced by 61.49% for CD10 at 90%, by 3.78% for CD30 at 95.2%, and by 9.77% for CD60 at 99.67%. At a reaction time of 60 minutes, CD10 and CD30 samples seemed to exhibit more improvement in terms of TSS removal performance with 7.41% for CD10 at 96.67% and by 3.5% for CD30 at 98.53%. As for CD60 a slight decline which was estimated by 0.8% in the TSS removal percentage. This enhancement in TSS removal pattern and their corresponding removal was reported by several authors. (Phalakornkule et al., 2010) This improvement could be correlated due to the charge neutralization mechanism that tends to take place more effectively with the longer reaction time and the

higher current density, resulting in an increase in the coagulant formation rate, and hence increasing the TSS removal rate. (Rahmalan, 2009).

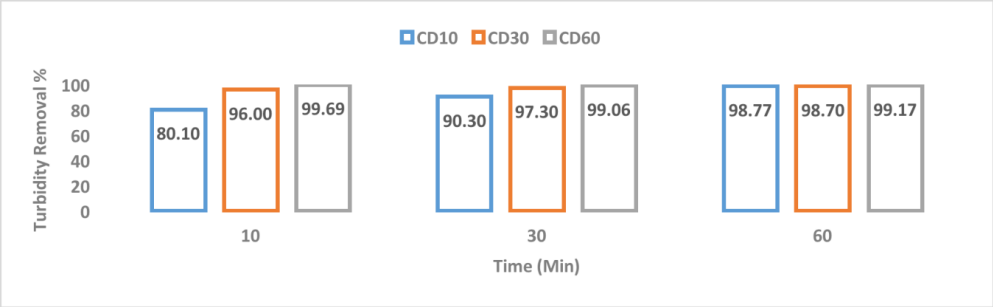

Figure 16: Turbidity removal for 3 pure samples at different current densities at different timelines

The turbidity removal for these 3 pure samples is illustrated in Figure 16. As seen, The CD10 sample showed a 80.1% turbidity removal percentage after a 10 minutes reaction time, and as the time reached 30 minutes, a 90.3% removal was achieved for the same current density, leading to a 98.77% of turbidity removal after 1 hour of reaction time. The same trend are as the CD30 sample where the turbidity removal percentage was 96%, 97.3%, and 98.7% for the time period of 10 ,30, and 60 minutes, correspondingly. It's worth mentioning that no major improvement was recorded in the turbidity removal at a high current density due to the rapid hydrogen formation on the cathode breaking the flocs formed from the coagulation process as reported by Mollah et al. (2001).

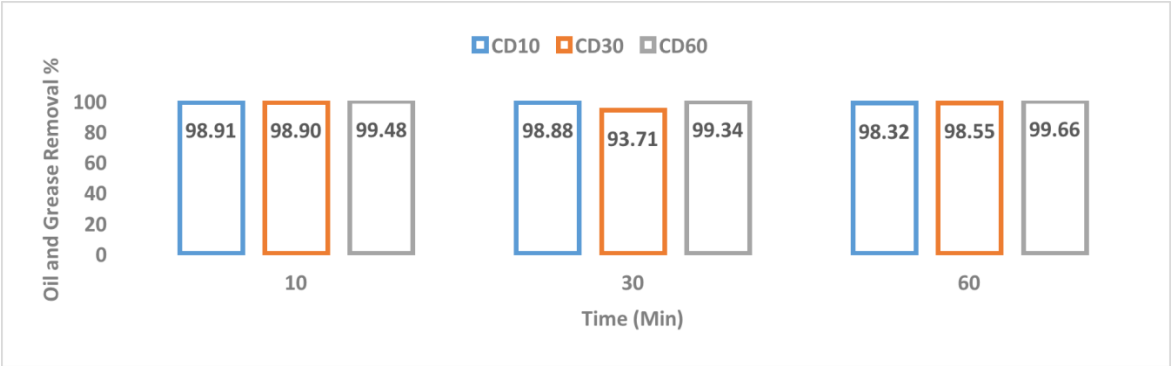

Figure 17: Oil and grease removal for 3 pure samples at different current densities at different timelines

As for Figure 17 , oil and grease removal percentage is illustrated for the same 3 samples, each at different current density. The percentage of removal is very for all the sample exceeding 98%. At 10 minutes' reaction time, the oil and grease removal achieved for the sample were as follows: CD10:98.91%, CD30:98.8, and CD60 99.48. As it can be noticed that as the current density increases at a 10 minutes' timeline, the removal is seen to improves as well. After 30 minutes of reaction time the oil and grease removal remained the same for all sample except for the CD30 where the removal reached 93.7%. After 60 minutes of reaction time all the sample removal percentage reached over 98.5% except for the cd10 sample which dropped to 98.32%.As it can be observed that as the higher the current density reaches the higher the oil and grease removal occured which makes CD60 at a 60 minutes' reaction time being the highest removal at a 99.7% removal. It's worth mentioning that the variation amongst all the oil and grease removal percentage is almost similar, at 10 minutes of reaction time. This results relates to the result reported by Ayhan which indicated that after a longer reaction

time at a certain current density, an optimum oil and grease removal is achieved, and that the higher the current density , the faster the ability to reach that optimum removal point.(Şengil & özacar, 2006)

3.1.2. Effect of reaction time

The effect of the reaction time of the pure samples against the current density on the total suspended solids, the turbidity and the oil and grease removal percentage was studied and shown in the figures below.

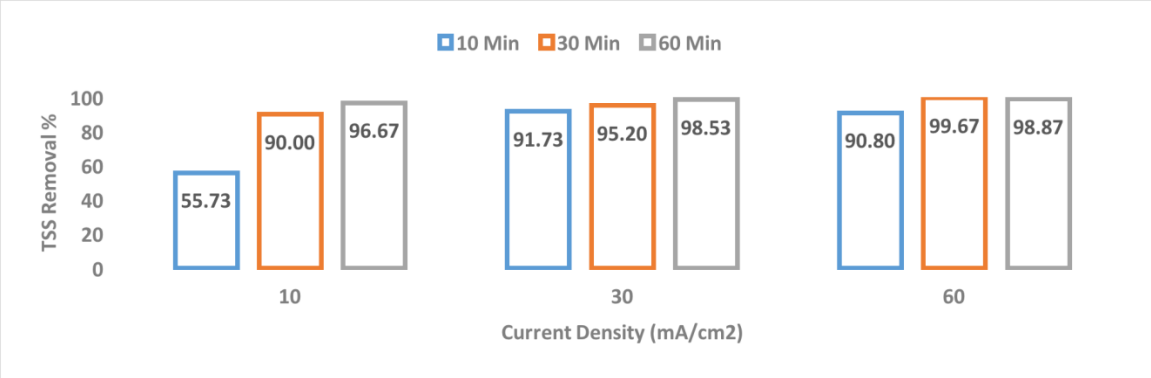

Figure 18: TSS removal for 3 pure samples in reaction times at different Current Densities

Figure 18 shows the relationship of 3 samples containing pure sample .The run time was studied was carried out at a certain current density ranging between 10 , 30 and 60 mA/cm^2 and at different reaction times ranging between 10 , 30 and 60 minutes. At a current density of 10 mA/cm^2, the sample with a reaction time of 60 minutes is achieving the highest TSS removal at a 96.67% removal was achieved, when compared with 30 minutes and the 10 minutes' reaction time samples, at a 90% and 55.73% removal

percentage respectively. As the current density increases to 30 mA/cm^2, an average of 24% overall improvement in TSS removal is achieved for all sample with the improvement percentage of: 10 minutes' reaction time: 64.6% improvement, 30 minutes' reaction time:5.78% improvement, and 60 minutes' reaction time :1.92% improvement. At a current density of 60 mA/cm^2, the TSS removal is enhanced slightly for the sample run of 30 and 60 minutes resulting in a 99.67% and 98.87% TSS removal respectively, while the 10 minutes' sample having a lower removal than when at a current density of 30 mA/cm^2 at a 90.8% TSS removal.

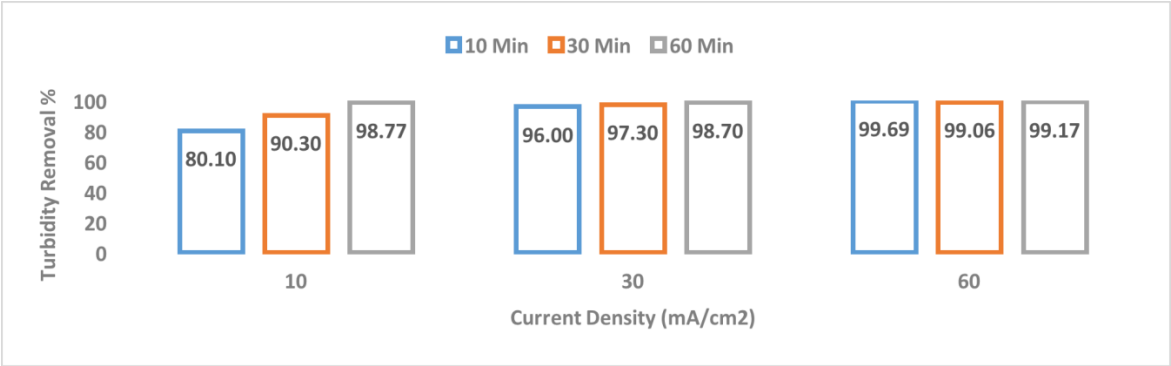

Figure 19: Turbidity removal for 3 pure samples in reaction times at different Current Densities

Figure 19 shows the turbidity removal for the same 3 sample shown in Figure 18. In the figure it can be seen that at a current density of 10mA/cm^2 the turbidity removal was 80.1% at a 10 minutes' reaction time, and the removal percentage increased as the reaction time increased reaching 90.3% at a 30 minutes' reaction time, and 98.77% at a 60 minutes' reaction time. As the current density reached 30 mA\cm^2, the turbidity

removal percentage started to stabilize to reach an average removal of 97% with 60 minutes reaction time being the highest at a 98.7% and the 10 minutes reaction time being the lowest at a 96%. At 60 mA/cm^2 , all the reaction time samples seemed to have a similar turbidity removal at 99% with small variation between the sample of a value of 99.35±0.25.

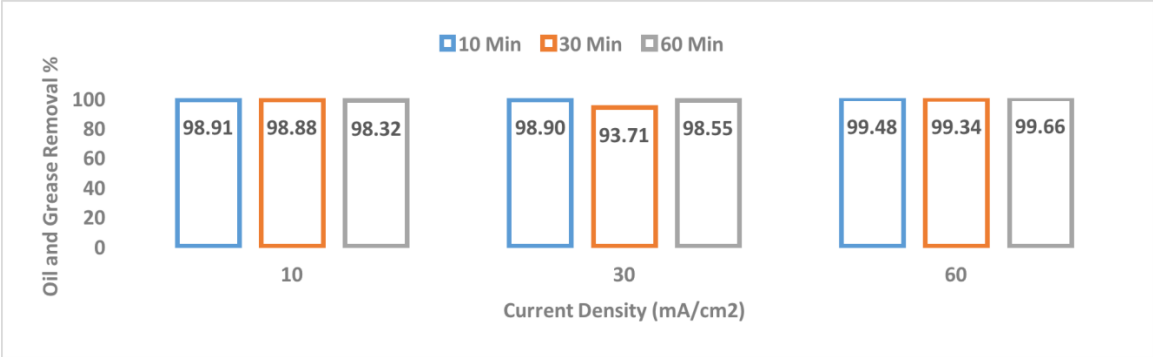

Figure 20: Oil and grease removal for 3 pure samples in reaction times at different Current Densities

The oil and grease removal percentage is illustrated in Figure 20. Overall variation amongst all samples at all current densities and all reaction times seemed to exhibit a similar performance, as in the case of the oil and grease removal with the samples run at 60 mA/cm^2 had the highest oil and grease removal at a 99.66% for the 60 minutes' reaction time and a lowest value at a 30 minutes reaction time at a 99.34%, while the rest of the samples at 10 and 30 mA/cm^2 had the same removal at all reaction times at an approximately 98% removal.

3.2. The slag sample performance

The total suspended solids, turbidity and oil and grease removal percentage was studied, for 6 slag containing samples, 3 of which were studied with variations in the current density ranging between 10, 30, and 60 mA/cm^2, and at different timelines, while the rest were studied by setting periods of reaction times ranging between 10,30, and 60 minutes, and at different current densities.

The addition of the steel slag contributed to the reactions taking place within the produced water. It's presence in the produced water tends to change the pH of the water initially slightly, then when not added. Furthermore, as the electrocoagulation reaction takes place in the water, initially the slag does not react as much as the anode and the cathode. However, as the reaction time and the current density change, various reactions start to take place within the produced water. These reactions are as follows (Şengil & özacar, 2006):

$$Fe_{(s)} \rightarrow Fe^{+2} + 2e$$

$$Fe^{+2} + 3H_2O \rightarrow Fe_2O_{3\,(s)} + 6H^+ + 2e$$

$$4Fe_{(s)} + 3O_2 \rightarrow 2Fe_2O_{3\,(S)}$$

$$Fe_2O_3 + 3ClO^{-1} + OH^{-1} \rightarrow 2H_2O + 3Cl^{-1} + 2{FeO_4}^{-2}{}_{(aq)}$$

$${2FeO_4}^{-2}{}_{(aq)} + 4H_2O + 3e \rightarrow Fe(OH)_{3\,(s)} + 5OH^{-1}$$

As seen from the reactions, one of the products generated from the presence of the slag, is the OH. This results in changing the pH of the produced water to reach 7, which in return forms $Fe(OH)_3$ as illustrated in Figure 21. Its presence contributes in forming

and settling more sludge from the oil and grease particles present in the produced water. This takes place as a result of the diffusion process of the Al and Fe ions through the double layer formed around the oil and grease colloidal particles, which in turn reduces the electrical double layer as well as the repulsive forces between the oil particles, leading them to settle down.

Another process that takes place in the presence of the slag in the produced water is the sweep coagulation process. This process takes place as a result of the metal salts formation, which forms insoluble metal hydrates. This metal hydrate causes a sweep electrocoagulation process and precipitates and forms a sludge layer in the solutions. An overall view of the electrocoagulation process in the produced water in the presence of the slag can be seen in Figure 23.(D. Ghernaout, Naceur, & Ghernaout, 2011).More over the flocculent formed because of the EC reaction can be visible in Figure 22 .

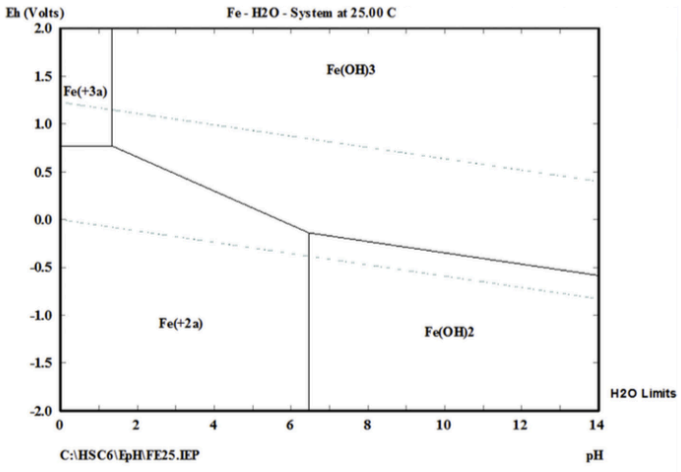

Figure 21: E-pH diagram of Fe at room temperature (Moussa et al., 2017)

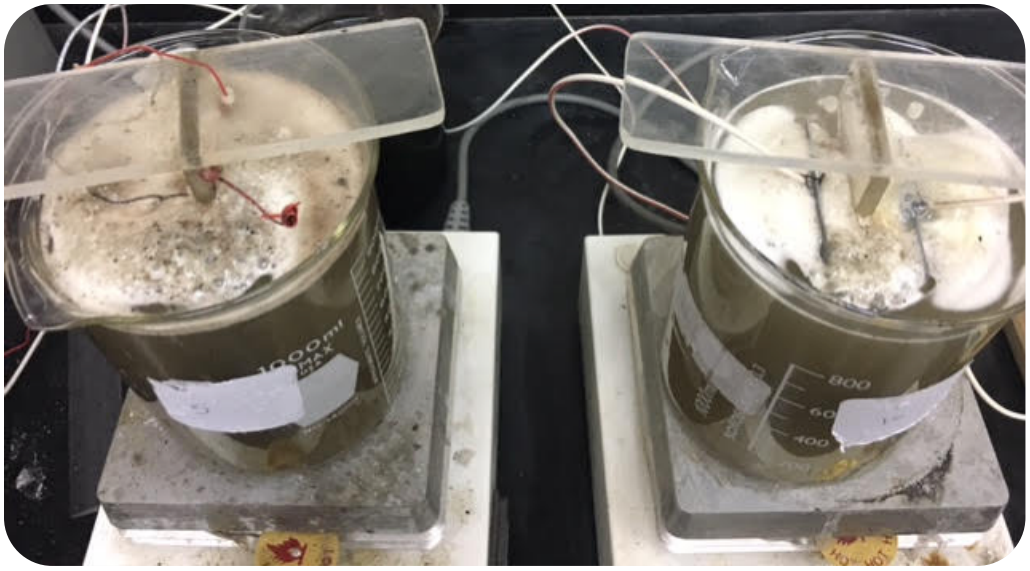

Figure 22: Pure and slag sample forming a flocculent layer after the EC process

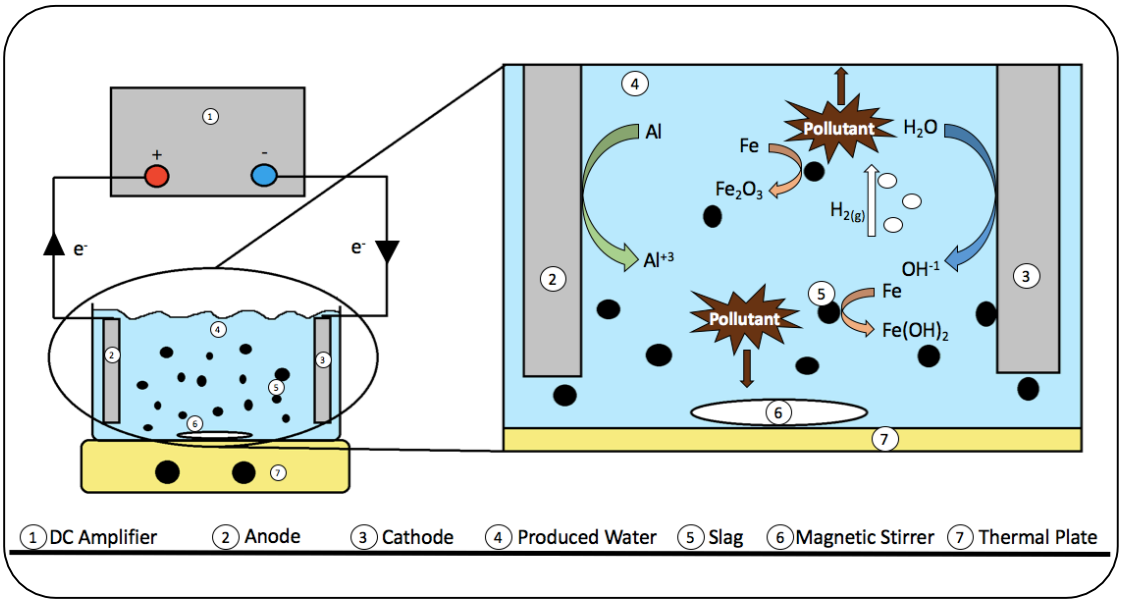

Figure 23: Overall electrocoagulation process in produced water in the presence of steel slag

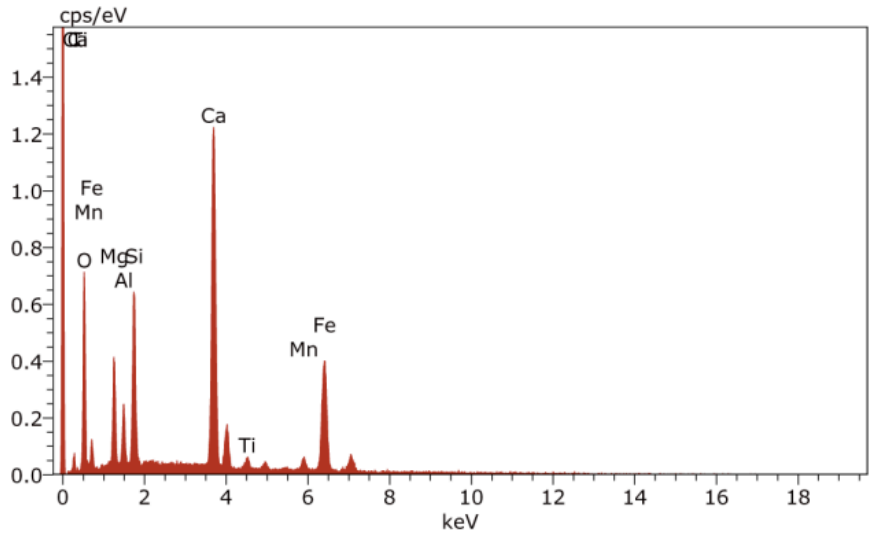

Figure 24: EDAX analysis of 425nm Slag sample prior EC Process

Figure 24 and Table 6 shows energy dispersive x-ray test and the elemental analysis for a slag sample of 425 nm particle size before EC process. In the data, the percentage of Fe is at a 21.7 % with a 36% of O in the sample indicating the presence of Fe_2O_3 in the sample. Also, Figure 25 shows the infrared spectrum for a slag sample of 425 nm particle size. The only where it can be seen that only the presence of Fe-O bond can be seen at 500 cm^{-1}.

Table 6*:*

EDAX analysis of 425nm Slag sample prior EC Process

Elements	Atomic Number	Atomic Weight %
C /Al	6 / 13	3.79 / 2.24
O	8	36.2
Mg	12	5.2
Si	14	5.53
Ca	20	22.53
Ti / Mn	22 / 25	1.1 / 1.72
Fe	26	21.7

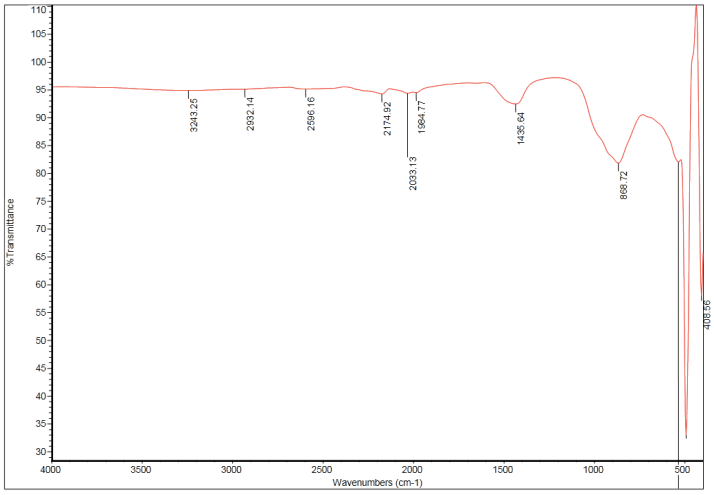

Figure 25: FTIR image of a slag sample prior EC Treatment

3.2.1. *Effect of current density*

The total suspended solids, turbidity and oil and grease removal percentage were studied, for 3 slag containing samples, each of which is set at a current density ranging between 10, 30, and 60 mA/cm^2, for a period of time of 10,30 and 60 minutes. This was achieved to assess the effectiveness of current density variation on the parameters' percentage of removal.

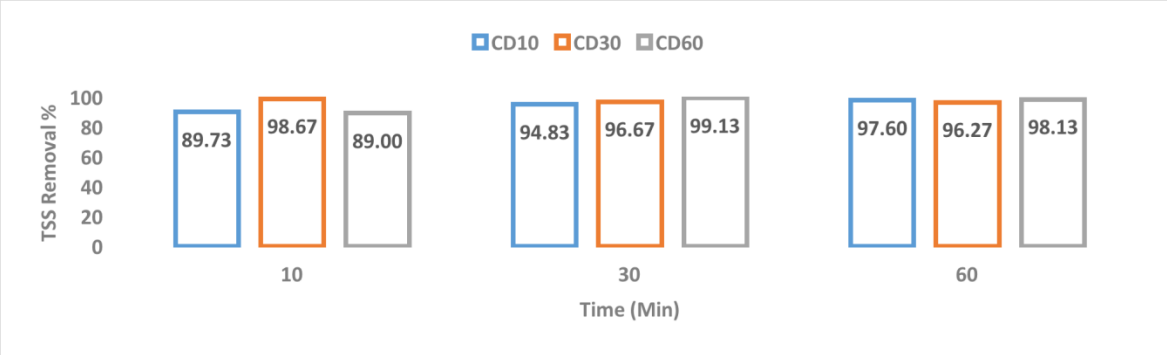

Figure 26: TSS removal for 3 Slag containing samples at different current densities at different timelines

Figure 26 shows the total suspended solids removal percentage in a 3 slag containing samples, each run at three time intervals ranging between 10, 30, and 60 minutes at different current densities of 10, 30 and 60 mA/cm^2. At 10 minutes' reaction time, CD60 sample is showed a lowest TSS removal with 89% removal, while the CD30 sample is showed the highest removal at 98.67%. As for the CD10 sample the removal percentage was 89.73%. As the reaction time reaches 30 minutes, the TSS removal percentage was enhanced by 5.68% for CD10 at 94.83% and by 11.38% for CD60 at

99.13%. As for the CD30 sample, the TSS removal was decreased by 2% at a 96.67%. At a reaction time of 60 minutes, CD10 sample seemed to exhibit more improvement in terms of TSS removal performance by 3% for CD10 at 97.6%. As for the CD30 and CD60 samples, the removal declined slightly by 0.4% for CD30 at 6.27% and by 1% for CD60 at 98.13% in the TSS removal is noticed.

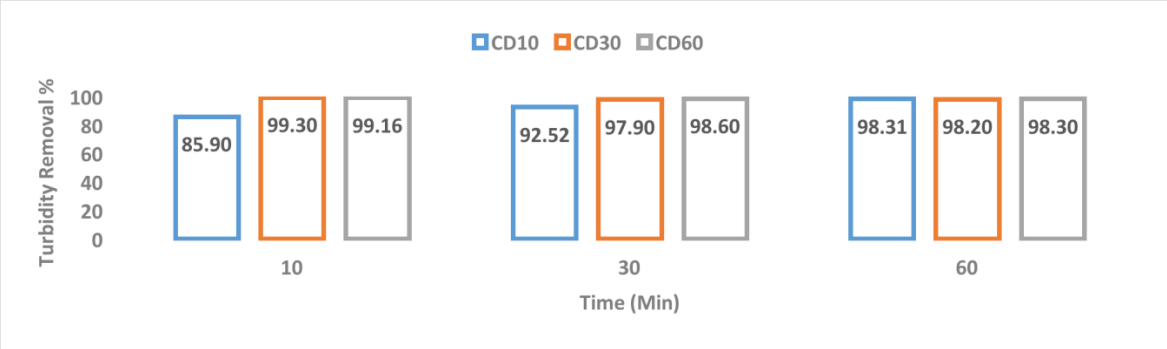

Figure 27: Turbidity removal for 3 Slag containing samples at different current densities at different timelines

The turbidity removal for these 3 pure samples is illustrated in Figure 27. As seen, The CD10 sample showed an 85.9% turbidity removal percentage after a 10 minutes' reaction time, and as the time reached 30 minutes, a 92.52% removal was achieved for the same current density, leading to a 98.31% of turbidity removal after 1 hour of reaction time. However, the same trend can't be said for the rest of the samples, where for the slag sample run at a current density of 30 mA/cm^2 and 10 minutes' runtime the turbidity removal was at a 99.3%, and as the time increase the removal percentage declined to a 97.9% after 30 minutes, then increased to reach 98.3% of turbidity removal

after 60 minutes. Similarly for the CD60 sample except that after 60 minutes' reaction time, the turbidity removal percentage remained the same.

The EDAX results show that the Fe particles react with the EC systems , which can be clearly seen in the decrease of the atomic weight of the Fe as shown in Figure 28 and Table 7 after the EC treatment process. From the data, the Fe percentage decreased reaching 20.3%, while the aluminum percentage was 1.6%, indicating that both the aluminum and the iron in the sample are removed by the EC process. This is further supported by the decrease in the O percentage to a 33.5%, indicating lesser presence of the Fe_2O_3 .

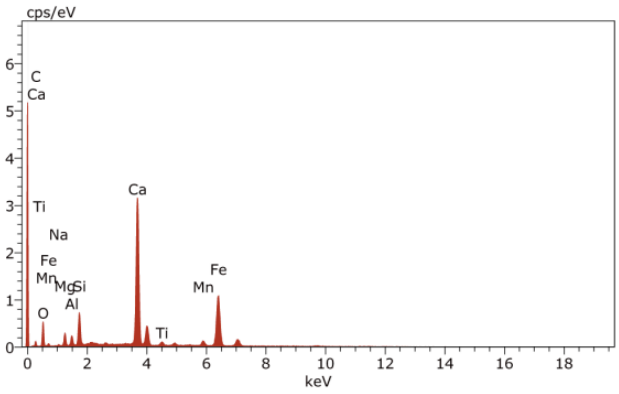

Figure 28: EDAX analysis of 425nm Slag sample after EC Process

Table 7*:*

EDAX analysis of 425nm Slag sample after EC Process

Elements	Atomic Number	Atomic Weight %
C	6	7.72
O	8	33.44
Na /Mg	11 / 12	0.4 / 3.1
Al / Mn	13 / 25	1.61 / 1.5
Si	14	4.84
Ca	20	26.2
Fe	26	20.3

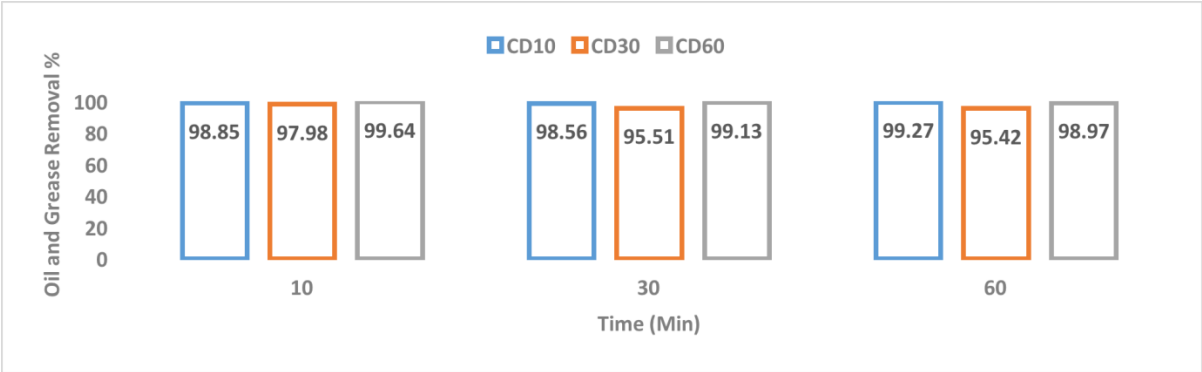

Figure 29: Oil and grease turbidity removal for 3 Slag containing samples at different current densities at different timelines

As for Figure 29, oil and grease removal percentage is illustrated for the same 3 slag containing samples, each at different current density. It can be seen that the percentage of removal is varies for the entire sample while exceeding a 95% removal. At 10 minutes' reaction time, the oil and grease removal achieved for the sample were as follows: CD10:98.85%, CD30:97.98, and CD60 99.64. As indicated the current density increases at a 10 minutes' timeline, the removal is an enhancement well, with an exception for the CD30 sample. After 30 minutes of reaction time the oil and grease removal remained almost the same for the CD10 sample. As for the CD30 and CD60 samples, the removal decline to 95.51% and 99.15% respectively. After 60 minutes of reaction time same trend remained consistent with an increase in the oil and grease removal for the CD10 sample at 99.27%, and with a decline for the CD30 and CD60 samples at a value of 95.42% and 98.97% respectively.

3.2.2. Effect of reaction time

The effect of the reaction time of the slag containing samples against the current density on the total suspended solids, the turbidity and oil and grease removal percentage were investigated.

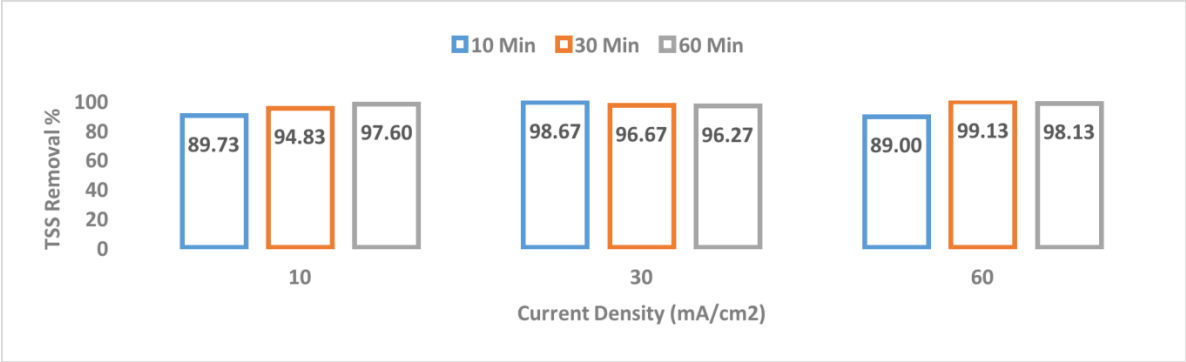

Figure 30: TSS removal for slag containing samples in reaction times at different current densities

Figure 30 shows the relationship of 3 slag containing samples, each run at a certain current density ranging between 10, 30 and 60 mA/cm^2 at different reaction times ranging between 10 , 30 and 60 minutes. At a current density of 10 mA/cm^2, the sample with a reaction time of 60 minutes achieved the highest TSS removal at a value of 97.6% removal, when compared with the 30 minutes and the 10 minutes' reaction time samples, at a 94.83% and 89.73% removal percentage respectively. As the current density increased to 30 mA/cm^2, both of the 10 minutes and the 30 minutes' reaction time samples seemed to exhibit improvement in the TSS removal percentage at a 98.67% for the 10 minutes' sample and at a 96.67% for the 30 minutes' sample. As for the 60 minutes' sample a slight decline was seen with a 96.27% removal. At a current density of 60 mA/cm^2 , the TSS removal is enhanced slightly for the sample run of 30 and 60 minutes with a 99.13% and 98.13% TSS removal respectively , while the 10 minutes sample had a lower removal than when at a current density of 30 mA/cm^2 at a 89% TSS removal.

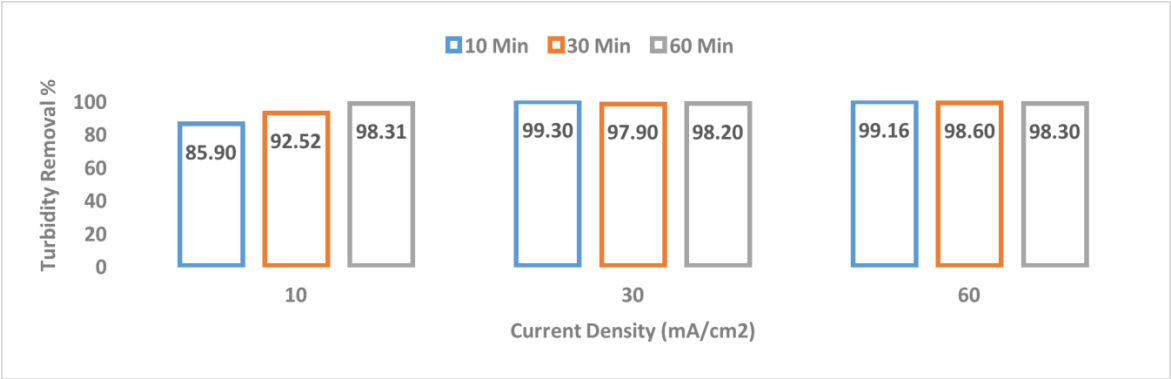

Figure 31: Turbidity removal for slag containing samples in reaction times at different current densities

Figure 31 shows the turbidity removal for the same 3 slag containing samples shown in Figure 30 . In the figure, it can be seen that at a current density of 10mA/cm^2 the turbidity removal was 85.9% at a 10 minutes' reaction time, and the removal percentage increased as the reaction time increased reaching 92.52% at a 30 minutes' reaction time, and 98.31% at a 60 minutes' reaction time. As the current density reached 30 mA\cm^2, the turbidity removal percentage started to stabilize to reach an average removal of 97%, at a10 minutes reaction time having the highest at a value of 99.3% at 30 minutes' reaction time having the lowest at a 97.9%. At 60 mA/cm^2 , all the reaction time samples seemed to have a similar turbidity removal at 98% with small variation between the samples of 98.6±0.35

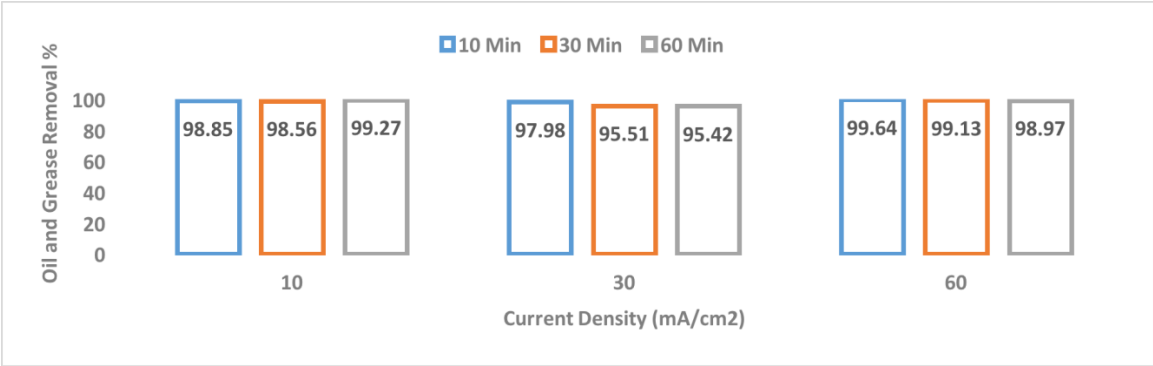

Figure 32: Oil and grease removal for slag containing samples in reaction times at different current densities

The oil and grease removal percentage is illustrated in Figure 32. Overall variation amongst all samples at all current densities and all reaction times seemed to exhibit a similar performance, with the samples run at 60 mA/cm^2 had the highest oil and grease removal at a 99.97% for the 60 minutes reaction time and the lowest value at a 30 minutes reaction time at a 99.13%, while the rest of the samples at 10 and 30 mA/cm^2 having the same removal at all reaction times at an approximated 98% removal except for the sample of 30 minutes and 60 minutes run at CD30 had a a removal percentage of 95.51% and 95.42% respectively.

3.3. The comparison of the slag sample and the pure sample

Several parameters were studied to evaluate and assess the performance of the slag containing sample against the pure sample in the electrocoagulation process, such as, the current density, the reaction time and the weight of the slag added to the pure sample.

3.3.1. *Effect of current density*

The effect of current density on the slag containing sample and the pure one, was studied for several factors such as the total suspended solid, the turbidity and the oil and grease removal as illustrated in figure 33. The relationship was studied to evaluate the performance of a slag containing sample, and the removal percentage was achieved and compared by pure sample at the same and at different current densities versus other factors such as the anode consumption, the power consumption and the sludge volume formed, all while maintaining a constant reaction time of 10 minutes.

3.3.1.1. *Total suspended solids removal*

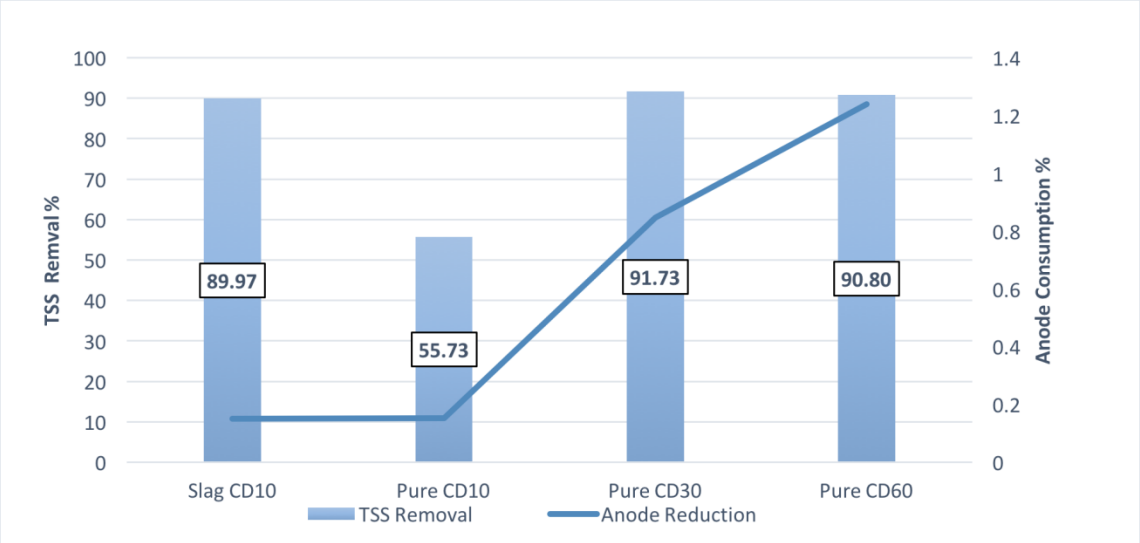

Figure 33: Total suspended solids removal at 10 min of reaction time under different current densities for different pure samples and for a slag sample of CD 10 against the anode consumption %

Figure 33 shows the relationship between total suspended solids removal and anode consumption, for four samples. These samples were a 5 grams' slag containing sample run at 10 mA/cm^2 current density, Three Pure samples, each of which is run at a different current density ranging from 10, 30 and 60 mA/cm^2. It was seen that at a 10 mA/cm^2 the slag sample provided a better TSS removal at an 89.97% removal, when compared with the pure sample run at the same current density, which achieved a 55.73% removal, all of which while maintaining less than 0.2% anode consumption to both cases. Furthermore, as the current densities increased for the pure samples, a better TSS removal percentage than that of the slag sample was achieved, at current densities of 30 and 60 mA/cm^2, where the removal percentage are 91.73% and 90.80% respectively (Elazzouzi et al., 2017). However, this enhanced TSS percentage of removal estimated by 1.8%, isn't worth mentioning considering the relatively high anode consumption (0.8% -1.24%) resulted at such current densities.

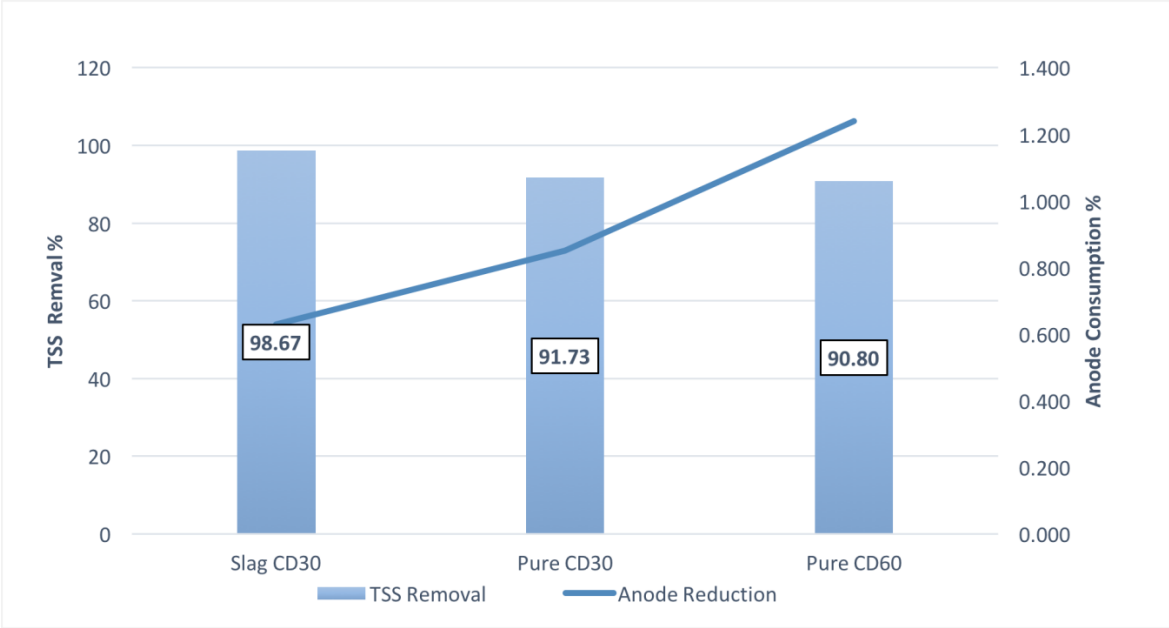

*Figure 34:*Total suspended solids removal at 10 min of reaction time under different current densities for different pure samples and for a slag sample of CD 30 , against the anode consumption %

Moreover, increasing the startup current density for the slag containing sample and the pure sample to 30 mA/cm^2, and then increasing it to a current density to 60 mA/cm^2 for the pure sample while measuring both the TSS removal and the anode consumption percentage resulted in Figure 34. An improved TSS removal percentage was seen for the slag containing sample than the pure sample at the same current density at 30 mA/cm^2 , while maintaining a lower anode consumption percentage. The slag containing sample showed a better TSS removal of 98.68 % than the pure sample of 91.73% and a better performance than the pure sample at a current density of 60 mA/cm^2 of 90.8%. This was accompanied by a better anode consumption percentage estimated by 0.63% for

the slag containing sample at a current density of 30mA/cm^2 , 0.85% for the pure sample at the same current density , and a 1.24% for the pure sample at a higher current density of 60 mA/cm^2 .

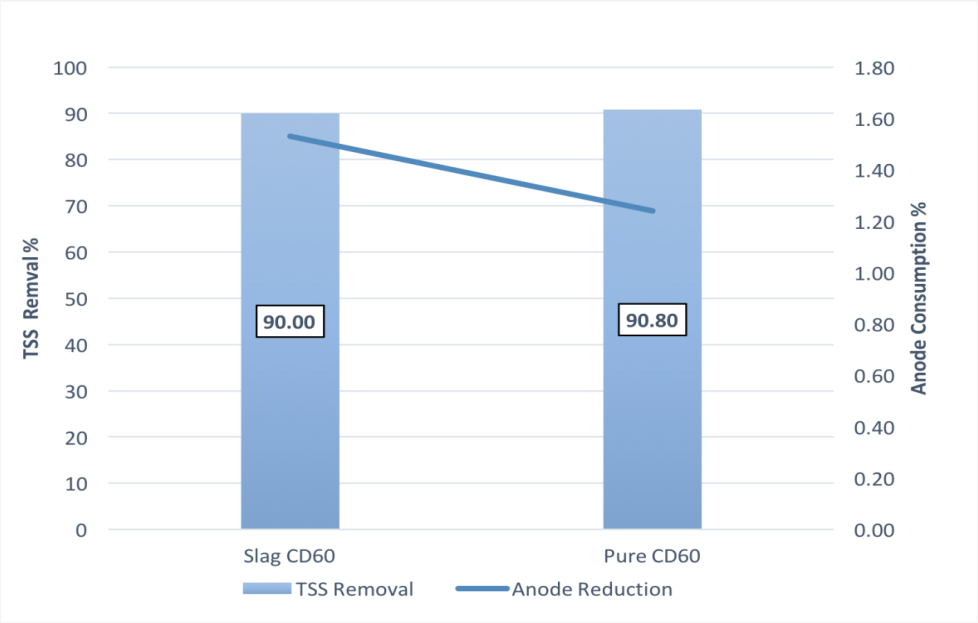

Figure 35: Total suspended solids removal at 10 min of reaction time under different current densities for different pure samples and for a slag sample of CD60 against the anode consumption %

The performance of , slag containing sample and a pure one at the same current density of 60 mA/cm^2 for 10 minutes compared as shown in Figure 35. It can be seen in the figure that the slag containing sample isn't a better improvement in TSS removal at a higher current density than the pure one with an estimated decrease of 0.8% difference than that of the pure sample. This decrease in the TSS removal is accompanied by an

increase in the anode consumption of 0.29% of that of the pure sample. This behavior indicates that at a higher current density, the slag will start reacting more with the anode causing the anode to be consumed more than that of the pure sample. This is to be explained in a section covering the relationship between the anode consumption and the current density in more details. The increase TSS removal for the slag containing sample over the pure sample can be best described by Schultze- Hardly's rule, which implies that the increase of the metal ions in the sample acts as a charge destabilizing agent for the colloidal particles , hence increase their settling chances .(Moussa et al., 2017). This is greatly noticed in the FTIR analysis

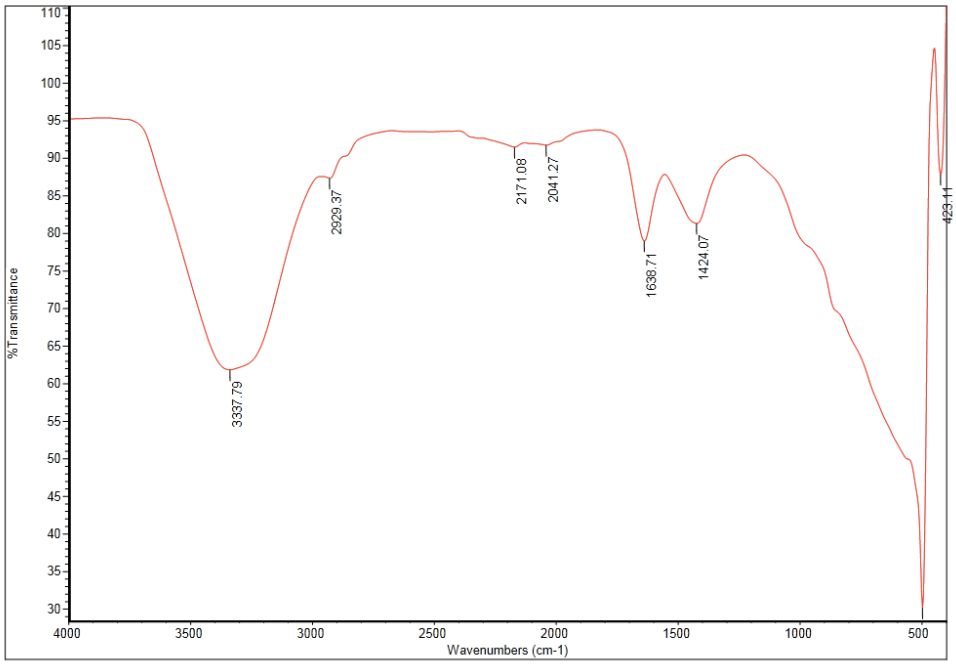

Figure 36: FTIR image of a slag sample after EC Treatment

As for Figure 36 , the slag sample was analyzed after an EC treatment process of 10 minutes reaction time, at a current density of 10 mA/cm^2 . The main functional groups is the hydroxide group at 3337 cm^{-1} stretch. This indicates the precedence of the $Fe(OH)_3$ resulted from the slag taking part in the electrochemical reaction with the anode and the produced water. Alongside these groups, the presence of the methyl (-C-H) functional group can be found at 1435 cm^{-1} as well. At 1630 cm^{-1}, the presence of an (H-O-H) bond can be found indicating the presence of water. The presence of Fe-O bond can be seen at 500 cm^{-1}.

3.3.1.2. Turbidity removal

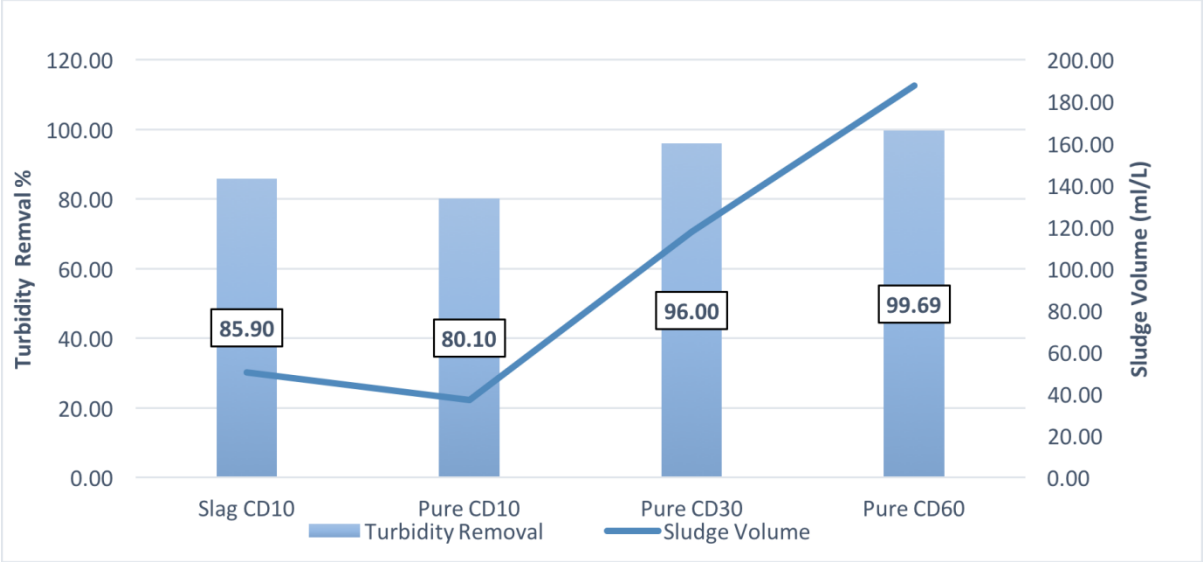

Figure 37: Turbidity removal at 10 min of reaction time under different current densities for different pure samples and for a slag sample of CD 10, against the sludge removal in ml/L

Another factor where the performance was tested as well, is the turbidity removal of the slag containing sample against pure sample at different current densities, while considering the volume of the sludge formed volume. Seen in Figure 37, The slag containing sample at a current density 10 mA/cm^2 showed a better turbidity removal performance at an 85.6% than the pure sample at the same conditions at 80.1%. However, this wasn't the case with the increase of the current density to 30 mA/cm^2 and 60 mA/cm^2 for the pure sample, which showed a better performance than the slag containing sample run at 10 mA/cm^2. The sludge volume formed is showed the same similar pattern to the turbidity removal pattern, where the slag containing sample is forming more sludge at 51 ml/L than the pure sample at 37 ml/L. This improvement however can be due to the volume of the slag within the imhoff cone, hence indicating an almost similar performance for the slag sample to the pure one at the same current density. The increase in the current density showed a great improvement over the sludge formed volume reaching 187 ml/L for the pure sample at a current density of 60 mA/cm^2. It's worth mentioning that the sludge layer formed from the electrochemical reaction, can be easily removed, considering the fact that it's mainly made of metal oxides.(Ghernaout, 2011). The deposition of these metals oxides can be seen in the SEM analysis. The SEM was used to identify the structure of the 425-nm particle size slag before and after the electrocoagulation process in order to identify where or not if any changes would occur to the slag structure and what sort of changes would occur. The figure below shows the differences of between two slag sample, each two at the same magnification scale, both before and after the EC process. Figure 38A and Figure 38B shows the slag sample at a

25k magnification before and after the electrocoagulation treatment correspondingly. In terms of structure, the slag sample prior treatment (A) seemed to be having a large colloids structure when compared to the same sample after the EC treatment (B), where these large collides tends to decrease into a smaller size. As for the boundaries between these particles, it can be seen that the slag sample prior treatment at a higher magnification of X50 in Figure 38C , tends to have large gaps in its structure when compared to the same sample after the treatment (D). The same thing can be said to the adhesion between the particles, where it is visible in Figure 38E at X100K magnification that the slag sample pre-treatment tends to be less uniform with every wide range of particle sizes. As for Figure 38D , the same sample after the EC treatment tends to have a small gaps between its particles due to the formation metal oxides between their particles, leading to more sludge formation in the presence of the slag.

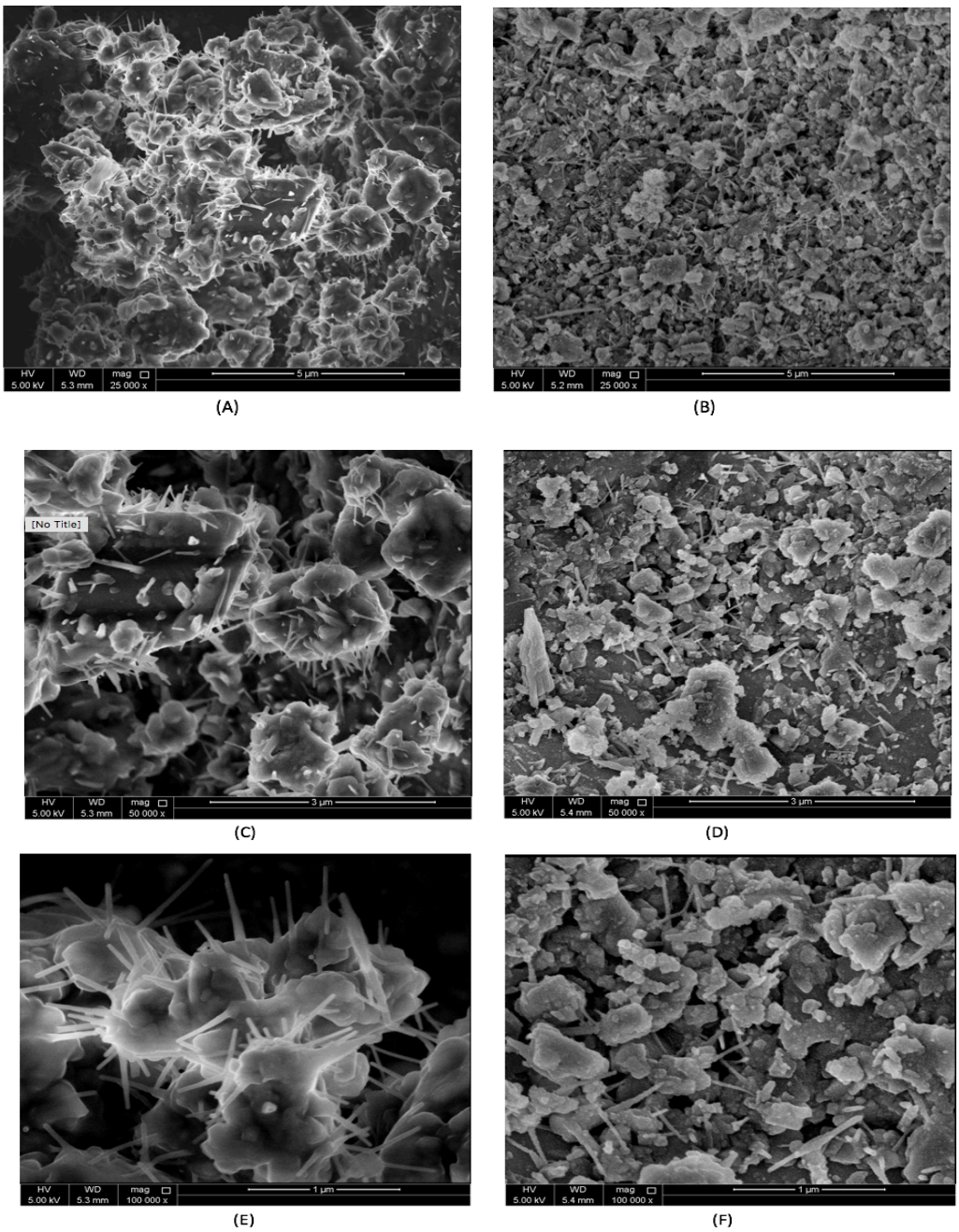

*Figure 38:*SEM images for 2 slag samples at different Magnifications A) Pre-EC Treatment at X25k. B) After EC Treatment at X25k. C) Pre-EC Treatment at X50k. D) After EC Treatment at X50k. E) Pre-EC Treatment at X100k. F) After EC Treatment at X100k

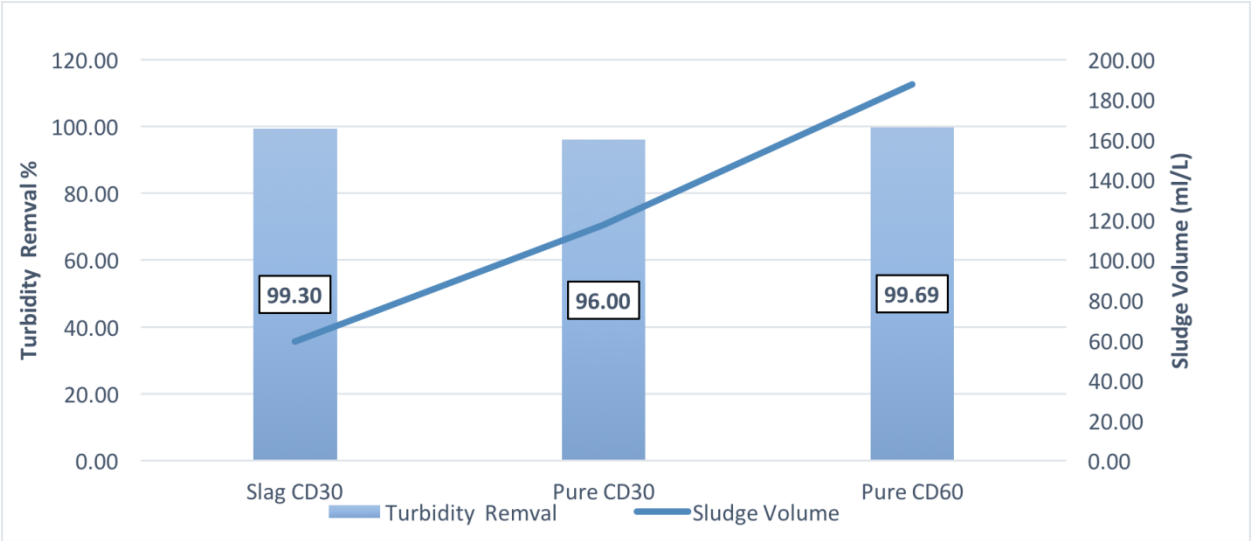

Figure 39: Turbidity removal at 10 min of reaction time under different current densities for different pure samples and a slag sample of CD 30 against the sludge removal in ml/L

As seen in Figure 39 ,the turbidity removal for the slag containing sample showed a better performance at the 99.30% removal than the pure sample at the same current density of 30 mA/cm^2, and a similar performance for the pure sample at a current density of 60 mA/cm^2 at a 99.7% removal. However, the slag containing sample seemed to show a worst performance at 60 ml/L when compared to the pure sample at 118 ml/L at the same current density.

Figure 40: Turbidity removal at 10 min of reaction time for a slag sample of and another pure sample at CD60 against the sludge removal in ml/L

At 60 mA/cm^{2,} the slag sample showed a similar turbidity removal performance to the pure sample at a 99% removal, while showing a far better sludge formation of 312 ml/L compared to the pure sample sludge volume of 187 ml/L as per Figure 40. This indicates that slag sample tends to form more sludge than the pure sample at a 60 mA/cm^2 current density.

3.3.1.3. Oil and grease removal

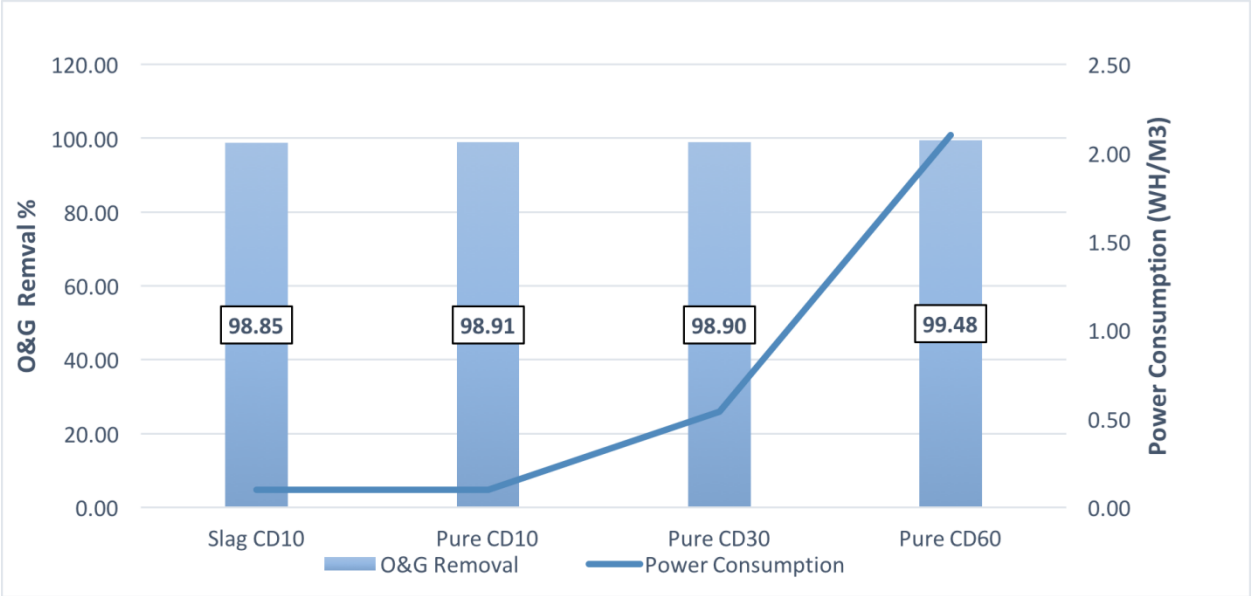

Figure 41: Oil and grease removal at 10 min of reaction time under different current densities for different pure samples and a slag sample of CD 10 against power consumption in WH/m^3

Illustrated in Figure 41, is the relationship between different samples run at different current densities, and their oil and grease removal percentage and its corresponding power consumption in WH/m^3. At a current density 10 mA/cm^2, both slag sample and the pure one showed a similar oil and grease removal percentage at a 98.8% and similar power consumption at 0.1 WH/m^3. As the current density increase for the other pure samples, the power consumption increases, while maintaining a similar oil and grease removal, extending to 99.5% at a 60 mA/cm^2. This concludes that the slag containing sample showed an overall better performance when compared with the higher

current density pure samples, and a similar performance to the same current density pure sample.

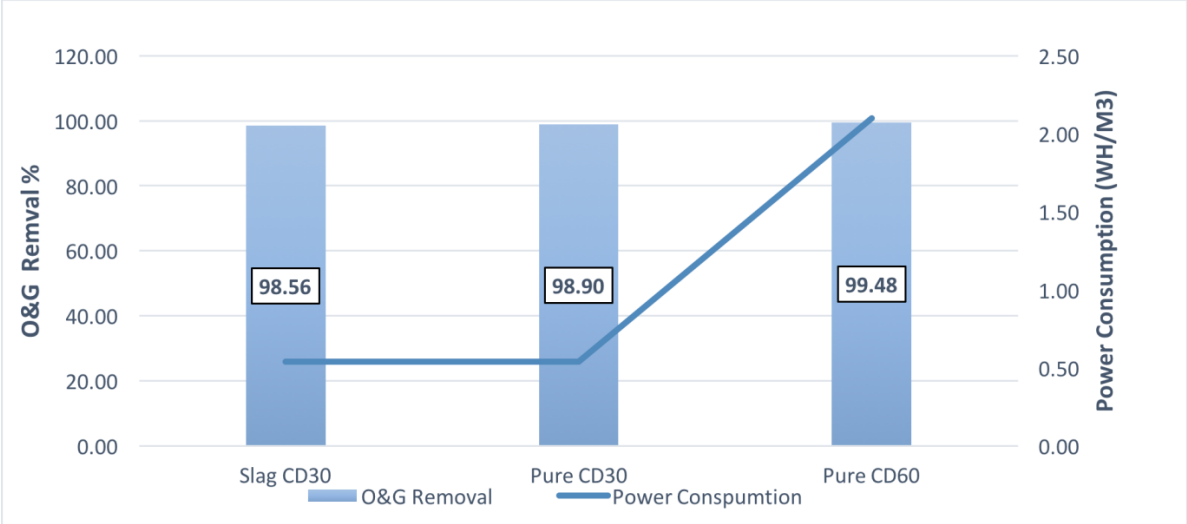

Figure 42: Oil and grease removal at 10 min of reaction time under different current densities for different pure samples and a slag sample of CD 30 against the power consumption in WH/m^3

In Figure 42, at a current density of 30 mA/cm^2 , the slag sample showed a similar oil and grease removal performance of 98.56% to the pure sample with a 0.5% enhancement to the pure sample , all while maintaining the same power consumption at a 0.54 WH/m^3. As the current density reaches 60 mA/cm^2 for the pure sample, an improvement in the oil and grease removal percentage can be noted reaching 99.5%. However, this improvement is contingent on the power consumption reaching 2.1 WH/m^3 , hence making the less than 1% oil and grease removal percentage difference from the slag sample not beneficial.

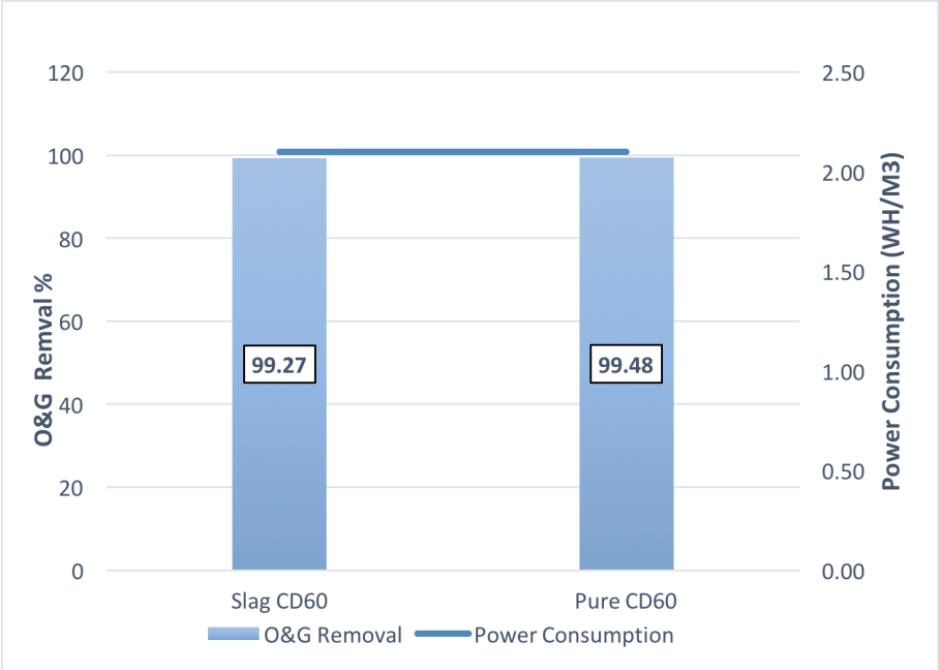

Figure 43: Oil and grease removal at 10 min of reaction time for a slag sample of and another pure sample at CD60 against the power consumption in WH/m^3

In Figure 43, at a current density of 60 mA/cm^2 , both of the slag sample and pure one showed an almost exact oil and grease removal percentage of 99.27% with a slight enhancement for the pure sample reaching 99.5% , while maintaining the same power consumption at a 2.1 WH/m^3

3.3.2. Effect of reaction time

The effect of reaction time on the slag containing sample and the pure one was studied for the same factors studied in the case of current density. The relationships illustrated show the performance of a slag containing sample, and compared it with a pure sample at the same and at different reaction times against other factors such as the

anode consumption, the power consumption and the sludge volume at a constant current density of 10 mA/cm^2.

3.3.2.1. Total suspended solids removal

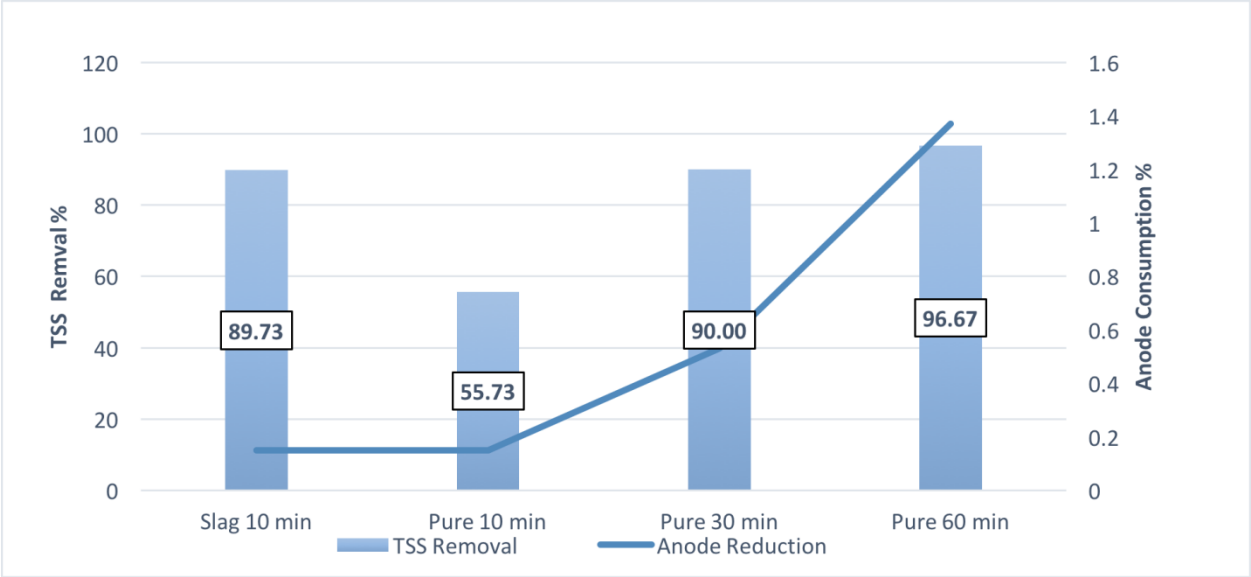

Figure 44: Total suspended solids removal at CD10 under different reaction times for different pure samples and for a slag sample reaction time of 10 min against the anode consumption %

Figure 44 shows the relationship between the reaction time, the total suspend solids removal percentage and the anode consumption for four different samples. One of which is a slag containing sample, and the rest are pure samples, each is run at different times, at the same current density of 10 mA/cm^2. After 10 minutes of reaction time, the slag sample achieved a better total suspended solid removal at a 89.7% than the pure sample at a 55.7%, while maintaining the same anode consumption of 0.15%. After 30

minutes of reaction time, the pure sample showed a similar performance of that seen by the slag sample after 10 minutes of a 90% TSS removal percentage at the cost of having a higher anode consumption at 0.53%. However, increasing the reaction time for the pure sample to a 60 minutes' run, increased its TSS removal percentage to 96.7%, while having a higher anode consumption of that of the slag sample at a 1.37%.

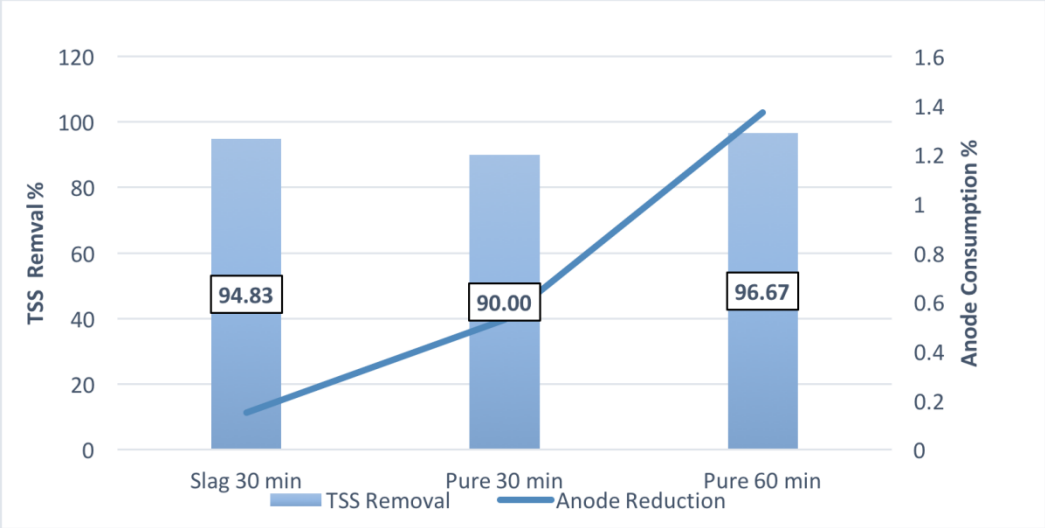

Figure 45: Total suspended solids removal at CD10 under different reaction times for different pure samples and for a slag sample reaction time of 30 min against the anode consumption %

In Figure 45, increasing the reaction time to 30 minute for both of the slag sample and the pure one, increased the slag sample TSS removal percentage to 94.83% over 90% for the pure sample, while having a lower anode consumption at 0.15% for the slag sample when compared to 0.53% for the pure sample. However, comparing the slag

sample run at 30 minutes to the pure sample run at 60 minutes, the slag sample showed a lower TSS removal percentage than the pure sample which has 96.67% percent, but at a high anode consumption of 1.37% .

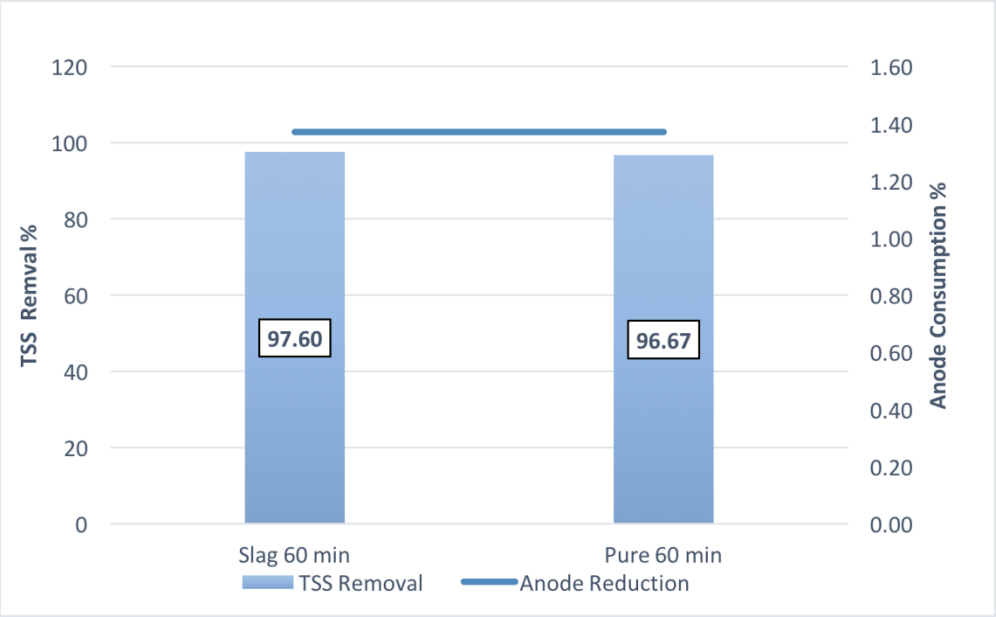

Figure 46: Total suspended solids removal at CD10 and a reaction time of 60 min for both of the slag sample and the pure sample against the anode consumption %

In Figure 46, setting the reaction time at 60 minutes for both of the slag and the pure sample, the slag sample proved superior to the pure sample in terms of TSS removal with a 97.6% for the slag sample and 96.67% TSS removal for the slag sample, all while having the same anode consumption of 1.37% for both samples.

3.3.2.2. Turbidity removal

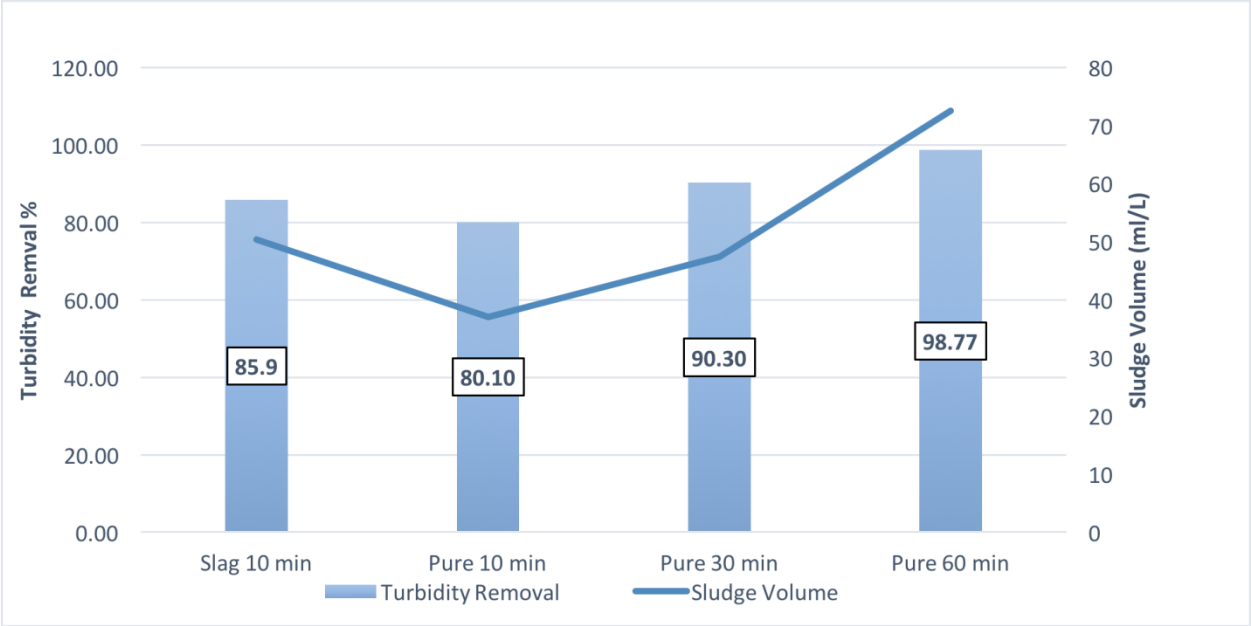

Figure 47: Turbidity removal at CD10 under different reaction times for different pure samples and for a slag sample reaction time of 10 min against sludge volume in ml/L

In Figure 47, the performance for turbidity removal of the slag containing sample against the pure sample at different reaction times was tested at a fixed current density of 10 mA/cm^2, while considering the volume of the sludge formed. The figure shows testing the turbidity removal percentage and the sludge volume (mL/L) for a slag sample at a 10 minutes reaction time, and comparing it to three pure samples, each of which is run at a different reaction time ranging from 10, 30, and 60 minutes. The slag sample showed a superior performance at an 85.9% turbidity removal compared to the pure sample run at 10 minutes' 80.1% turbidity removal, while maintaining a better sludge volume formation at a 50 ml/L to 37 ml/L of that of the pure sample. However, as the reaction

time increases for the pure sample, a significant enhancement is achieved over the slag sample in terms of the turbidity removal and the sludge volume formation. For the Pure sample, at 30 minutes the turbidity removal is 90.3% at a 47.7 ml/L sludge volume formation, and at a 60 minutes reaction time the turbidity removal is 98.77 % at a 72 ml/L sludge volume formation. It's worth mentioning that the high sludge volume formed and the high turbidity removal percentage is achieved at a long reaction time when compared to the slag sample run at 10 minutes. This difference is to be seen in the scenarios below.

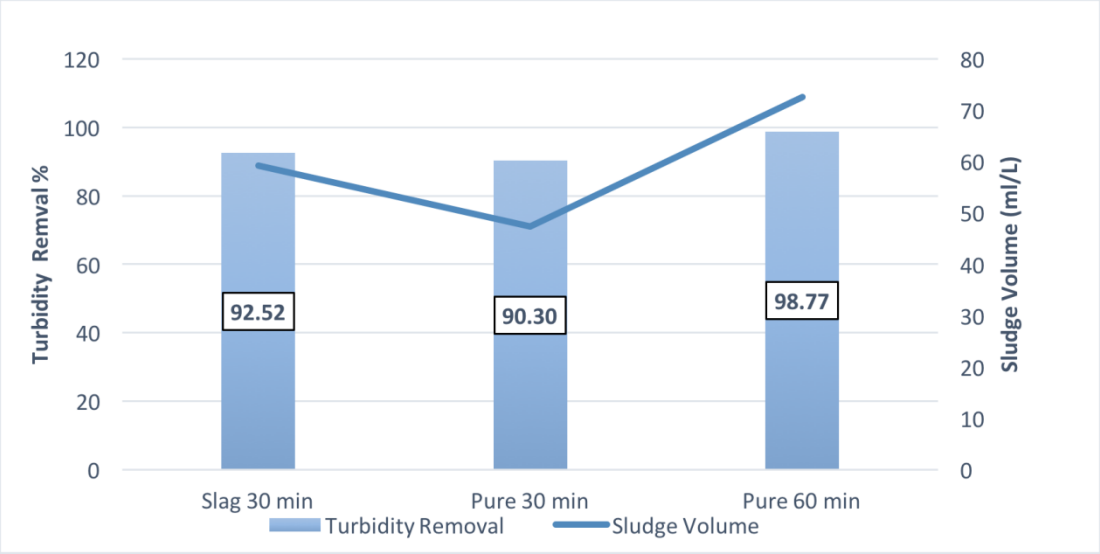

Figure 48: Turbidity removal at CD10 under different reaction times for different pure samples and for a slag sample reaction time of 30 min against sludge volume in ml/L

In Figure 48, increasing the reaction time to 30 minute for both of the slag sample and the pure one, increased the slag sample turbidity removal to 92.52% over 90.3% of

the pure sample, while having a higher sludge volume of 60 ml/L for the slag sample compared to 47 ml/L for the pure sample. However, comparing the slag sample run at 30 minutes to the pure sample run at 60 minutes, the slag sample showed a lower turbidity removal percentage than the pure sample which has 98.77% percent at a higher sludge volume of 72.6 ml/L.

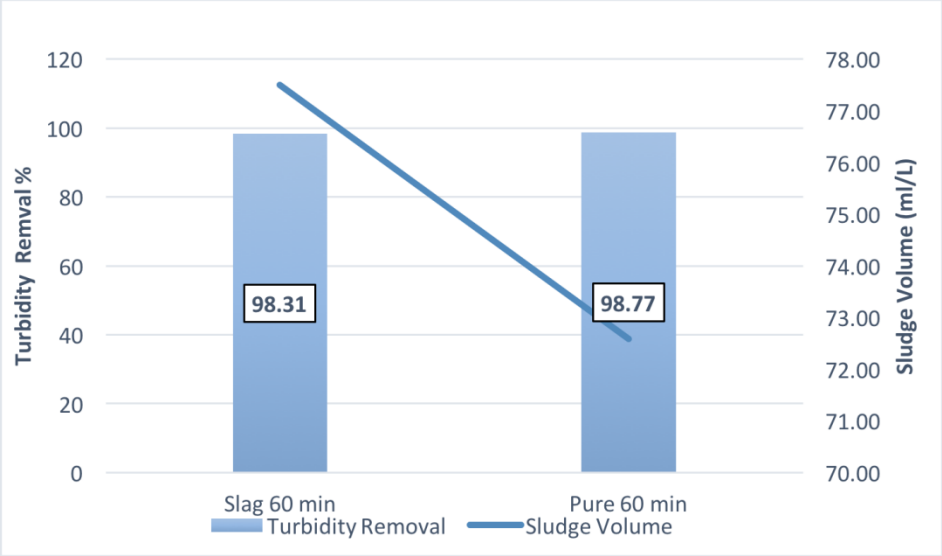

Figure 49: Turbidity removal at CD10 and a reaction time of 60 min for both of the slag sample and the pure sample against the sludge volume in ml/L %

In Figure 49, setting the reaction time at 60 minutes for both of the slag and the pure sample, the slag sample showed a similar performance to that of the pure sample in terms of turbidity removal with a 98.31% for the slag sample and 98.77% for the slag sample, while having a higher sludge formation volume estimated by 77.5 ml/L.

3.3.2.3. Oil and grease removal

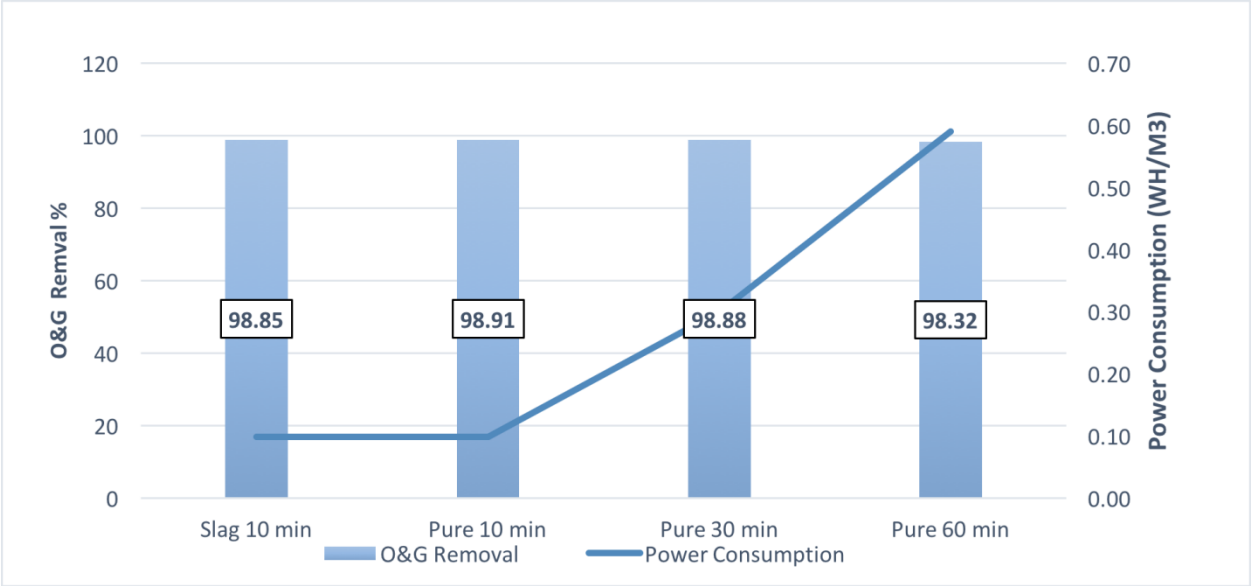

Figure 50: Oil and grease removal at CD10 under different reaction times for different pure samples and for a slag sample reaction time of 10 min against the power consumption in WH/m^3

In Figure 50, the relationship between different samples reaction time at the same current density of 10 mA/cm^2 and their oil and grease removal percentage and its corresponding power consumption in WH/m^3 are illustrated. At all reaction times for all the samples, very small variation in the oil and grease removal percentages amongst the four samples can be seen. The slag sample and the pure samples showed a similar oil and grease removal percentage at a 98.85% for the slag sample run at 10 minutes. As for the pure sample, the oil and grease removal achieved was 98.91% for the 10 minutes' sample, 98.88% for the 30 minutes' sample, and 98.32% for the 60 minutes' sample.

However, a key factor differentiating between the all these sample was the power consumption with the slag and the pure sample run at 10 minutes having the lowest power consumption at a 0.1 WH/m^3, and the pure samples run at a 30 minutes and a 60 minutes reaction time having a higher power consumption at a 0.3 WH/m^3 and 0.59 WH/m^3 correspondingly.

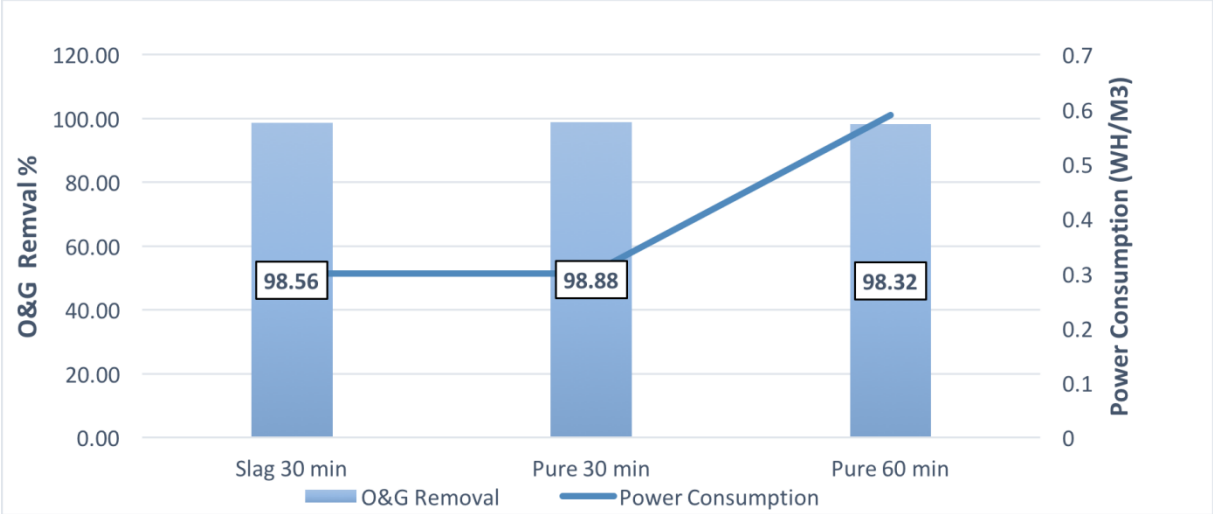

Figure 51: Oil and grease removal at CD10 under different reaction times for different pure samples and for a slag sample reaction time of 30 min against the power consumption in WH/m3

At a reaction time of 30 minutes as per Figure 51, the slag sample showed a similar oil and grease removal percentage removal performance of 98.56% to the pure sample with a 0.3% enhancement to the pure sample, all while maintaining the same power consumption at a 0.3 WH/m^3. As the reaction time reaches 60 minutes for the pure

sample, a slight decline in the oil and grease removal percentage can be noted, reaching 98.32% at the cost of having a higher power consumption of 0.59 WH/m^3.

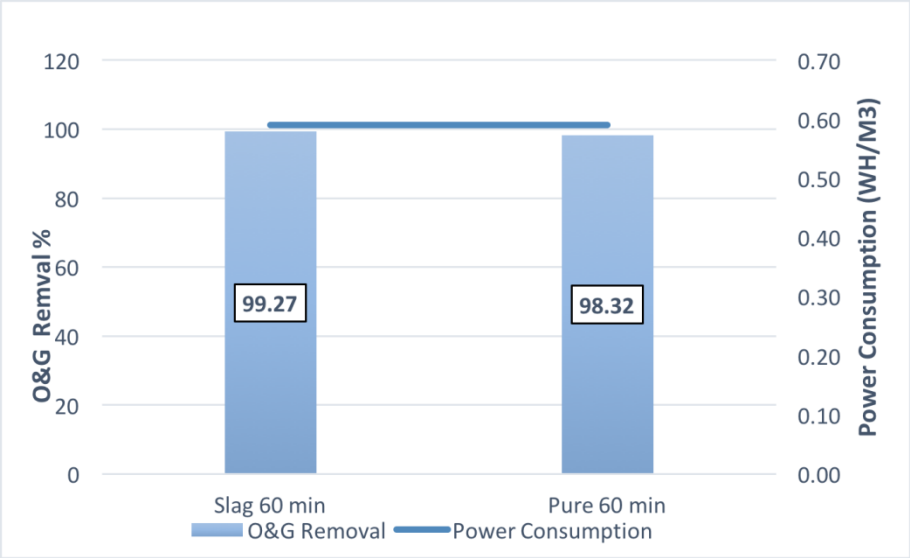

Figure 52: Oil and grease removal at CD10 and a reaction time of 60 min for both of the slag sample and the pure sample against the power consumption in WH/m^3%

In Figure 52, at a reaction time of 60 minutes, the slag sample seemed to preformed slightly better than the pure sample at 99.27% oil grease removal percentage, while the pure sample achieved a 98.32% removal, all while maintaining the same power consumption at a 2.1 WH/m^3

3.3.3. Slag Sample removal improvement over pure sample

As noticed from the sections above, a significant improvement of the slag containing sample is seen in terms of removal percentages of TSS, turbidity and oil and grease than the pure samples. This improvement can be explained by the adsorption

isotherm. In the pure sample the coagulation process tends to happen as a result of the aluminum hydroxide formation. As the electrochemical reaction takes place, aluminum hydroxide tends to form at 7 pH. These $Al_2(OH)_3(S)$ will tend to trap the pollutants and the colloids within the original sample and separate them in the form of sludge or foam. (Terrazas et al. , 2010)

The addition of the slag to the pure sample will cause the iron in the slag sample to start reacting with the system, transforming Fe^{+2} into $Fe(OH)_{3(s)}$ as well as $Fe(OH)_{3(aq)}$ alongside the aluminum hydroxide originally formed from the aluminum anode. These cationic hydroxides complexes will remove any pollutants by adsorption because of the charge neutralization, by complication, electrostatic attraction or by enmeshment in the form of Fe_2O_3 and $Fe(OH)_3$ precipitate. (Mollah et al., 2001)

Additionally, changes in pH value tend to take place as a result of the hydroxide species formation from 6 to 7.7 as indicated in the diagram below. This will cause improvement over the pure sample in terms of TSS, turbidity and oil and grease removal percentage.

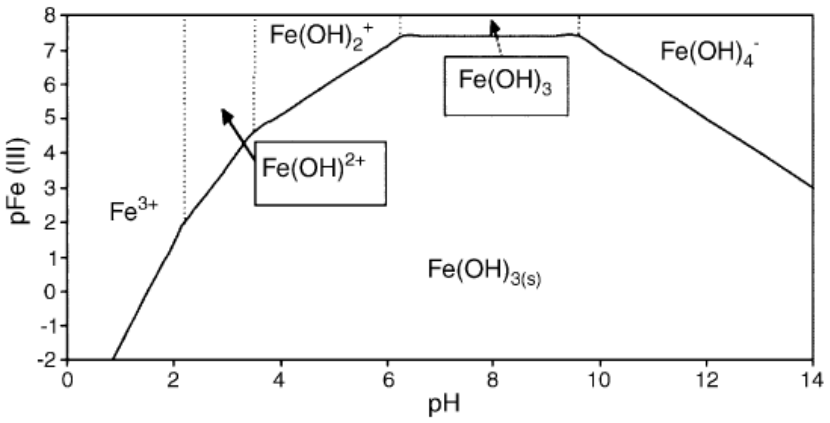

*Figure 53:*Dominance zone diagram for different Fe species at different pH (Ting & Dahlan, 2011)

Increasing either the current density or the reaction time beyond a CD30 mA/cm^2 or 30 minutes, reaction time showed a better removal for the pure sample in terms of TSS. However, the same can't be said for slag containing sample, where the adverse effect tend to happen most of the time. These adverse changes will effect both of the total suspended solids and the turbidity removal percentage, as well as the electrode consumption rate and the conductivity to a level lower than anything recorded in the case of the pure samples. This can be as a result of the decrease in the conductivity of the slag containing sample solution over the pure sample, due to the formation of Fe_2O_3 as seen in Figure 53, which in return affect the electrochemical cell efficiency and puts an extra load on the aluminum anode that is consumed at a faster rate.(Öztürk et al. , 2013)

3.3.4. *Effect of slag weight*

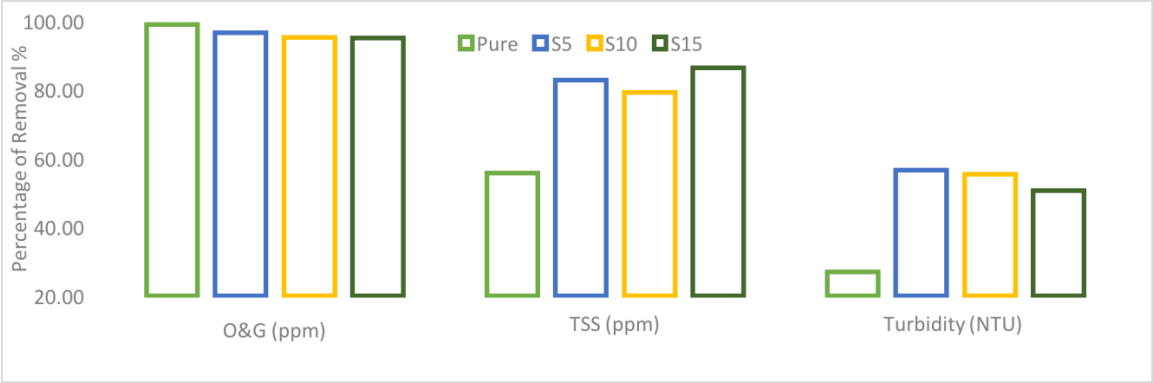

Figure 54: 3 slag samples of different weights of 5g, 10g, and 15g and a pure sample and the removal percentage for their TSS, o&g and turbidity for the same condition of CD10 at 10 min of reaction time

Figure 54 shows 3 slag samples of different weights of 5 grams, 10 grams, and 15 grams and a pure sample. The Removal percentage for their total suspended solids, oil and grease and turbidity removal is measured for the same condition of 10 mA/cm^2 current density at 10 minutes' runtime. The oil and grease removal is showed almost the same pattern for the four samples with a slight edge for the pure sample at a 99% removal over the slag containing sample, where at oil and grease removal percentage for the 5g,10g and 15g slag containing sample is 96.5%, 95.3% and 95% correspondingly. Furthermore, the total suspended solid removal percentage for the slag containing samples showed better removal with a minimal performance of 23.6% than the pure sample for the 10 grams' slag containing sample. Moreover, it's worth noticing that as the weight of the slag is increased, a better performance of 86% removal is seen, whereas

the 5 grams' slag containing sample showed an 83% TSS removal. However, this 3% difference of TSS removal percentage, isn't worth mentioning when considering the anode consumption, the turbidity removal percentage and oil and grease removal percentage, whom of which happens to increase for the anode consumption case, and decrease for the rest of the parameters. As for the percentage removal of turbidity, the slag containing sample showed a huge improvement over the pure sample, where the 5 grams' sample showed a 56% removal percentage, whereas the pure sample showed 27% of turbidity removal. With the increase of the slag weight, a decline was noticed in the turbidity removal, reaching 55% for the 10 grams' slag sample, and 50.6% for the 15 grams' slag sample. Overall, a better removal percentage was seen for the 5-grams' slag, and with any increase of the slag weight, a decline was seen. The reason for that can be either one of three things. The first reason can be that the addition of more slag to the produce water will cause the TSS and the Turbidity to increase due to the dust particle trapped within the slag pore. The second reason can be that the increase of slag weight will cause it to stick to the magnetic stirrer instead of spreading through the water, even at high a rpm. The third reason is due to the excess amount of slag added to the produced waster sample, an excess amount of Fe_2O_3, decreasing the current conductivity and hence decreasing the efficiency of the cell. Similar results were reported by Vepsäläinen (2012) indicating that the excess additional of any metals within the solution to be treated, is going to cause a reverse effect to the collides' stabilization process, affecting both of the turbidity and the total suspended solids removal.

3.4. Other factors

3.4.1. Current density and electrode consumption

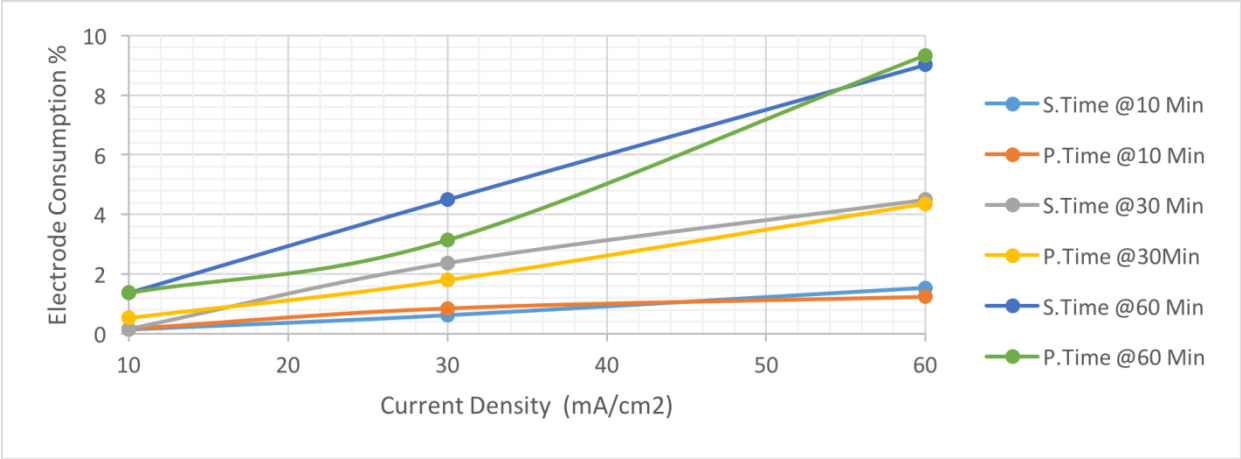

Figure 55: Current density Vs. electrode consumption for different slag and pure samples at different reaction times

Figure 55 shows the relationship between the electrode consumption and the current density for both pure water sample and the slag containing sample at different times. The relationship illustrated between the current density and electrode consumption is promotional, where the higher the current density achieved, the higher the electrode consumption reached. The same relationship can be said between the electrode consumption and the reaction time in general for both the slag containing sample and the pure sample. At a current density 10 mA/cm^2 at a 10 minutes' reaction time for both the slag containing sample and the pure sample, the electrode consumption is almost the same, unlike the case for sample runs at a current density of 30 mA/cm^2, where the slag

containing sample showed 0.5% electrode consumption less than the pure sample. Furthermore, the dramatic changes can be seen when running both samples at a current density of 30 mA/$cm^{2.}$ At a reaction time of 10 minutes, the Slag sample shows improved electrode consumption by 0.25% than the pure sample. However, as the reaction time increases, this result starts switching as a better performance is noticed for pure samples of 0.75% at 30 minutes and of 1.5% at 60 minutes than the sample containing slag. This can be explained by the fact that at the beginning of the electrochemical reaction in the slag containing sample, the AL-AL reaction will take place normally without any interference from the slag, yielding AL^{+3} and H^{+} within the solution. As the runtime increases, the pH of the solution will start changing and hence the E^{o} of the cell, changing the $Fe_{(s)}$ to $Fe^{+3}_{(aq)}$, $Fe^{+2}_{(aq)}$ $FeoH^{+}$ and other complex Fe species as per Nernst equation. These Fe species will tend to react with the anode electrons, when the slag is in direct contact with the anode to form solid Fe and hence becoming the another new cathode instead of the Al Cathode, resulting in a significant anode consumption of long periods of time.

3.4.2. *Conductivity and time relationship*

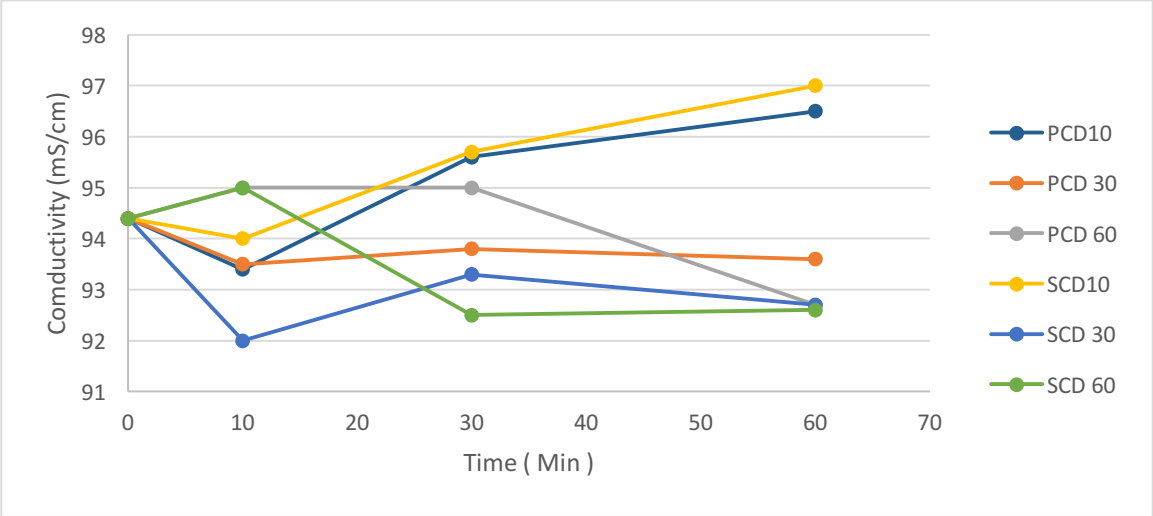

Figure 56: Conductivity vs. time for different pure and slag samples at different current densities

Figure 56 shows the current density variation for 6 samples, 3 of which are pure, and the others are slag containing samples. The differences between these samples lie within the variation of the current density. For each pure and slag containing sample, a 60 minutes run is achieved over an hour period, over 10, 30 and 60 mA/cm current density and the conductivity is recorded. The variation in conductivity can almost be random after 10 minutes for all the samples, followed by a steady state phase after 30 minutes until an hour run. The variation within the conductivity can be said to be insignificant, with the lowest conductivity recorded being 92 mS/cm and the highest at 97 mS/cm, keeping in mind that the original sample conductivity being at 94.3 mS/cm.

3.4.3. *pH and time relationship*

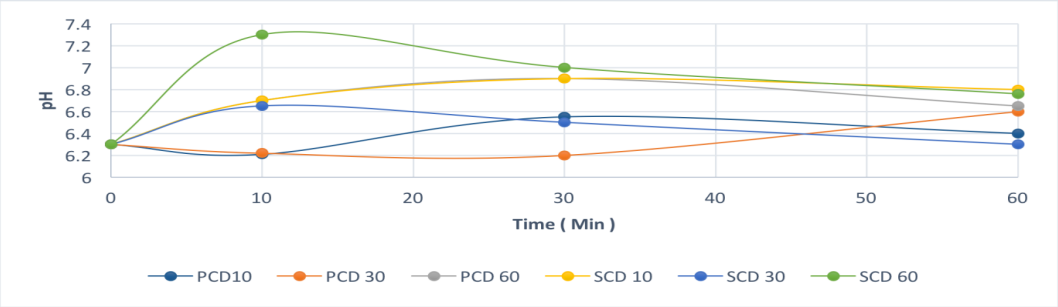

Figure 57: pH Vs. time for different pure and slag samples at different current densities

Figure 57 shows the relationship between pH change and the reaction time for different pure and slag containing samples at different current density. The variation seen in the pH for the different samples with time can almost be said to be random variation. This is due to the complex chemical reaction taking place in the sample as well as the high conductivity of the solution. (Chen, 2004) Moreover, at a current density 10mA/cm^2 the slag containing sample will tend to have a higher pH increase than the pure sample. This is almost the same case at a current density of 30 mA/cm^2, except for the fact that after 10 minutes the slag containing sample pH will tend to decrease below the pure sample pH at 60 minutes. At a current density of 60 mA/cm^2 both the slag and the pure sample exhibit the same pH variations. It's worth mentioning that the best removal efficiency's is found to samples of which initial pH is near neutral conditions and that the addition of slag to the sample is providing a way to remove any discoloration form the original sample (Fengxian et al.,1995) . This is due to the formation of yellow $Fe(OH)_{3(s)}$ particles at natural pH between 7-8 which replaces the black produced water particles.(Ghernaout et al., 2008)

CONCLUSION

The introduction of the steel slag to the electrocoagulation process for produced water treatment holds potential to enhance the pollutants removal efficiency and the power consumption in the overall process. The performance of total suspend solids, turbidity, and oil and grease removal percentage was studied for slag containing samples against pure samples amongst other characteristics such as the anode consumption, the electrolysis power consumption as well as the sludge volume formed. Key parameters that were controlled are the current density of the cell, the reaction time of the electrochemical reaction, as well as the slag weight. Controlling the current density was achieved by setting a constant reaction time of 10 minutes for all electrochemical reactions of both of slag containing samples and the pure ones, where it was seen that the slag sample provided a better TSS and turbidity removal percentage when compared with the pure sample at the same reaction time, while maintaining the same anode and power consumption and a better sludge formation volume. As for the oil and grease removal, the slag samples showed a similar performance to the pure samples when run at the same time period with a slight edge for the pure sample estimated by 0.3% oil and grease removal. Moreover, controlling the reaction time, while setting a constant current density at a 10 mA/cm^2 for all slag samples and the pure ones, where it was found that the slag sample increased the TSS removal with an average of 10% of that of the pure sample run at the same reaction time, while providing a similar anode consumption. As for the turbidity removal, at the same reaction time the slag sample showed an improvement in the removal percentage over the pure sample estimated at an average of 2.5%, while

having a higher sludge formation volume. As for the oil and grease removal, the slag samples showed a similar performance to the pure samples when run at the same time period, with a slight edge for the pure sample estimated by 0.15% oil and grease removal. Furthermore, controlling the weight of the slag at constant current density of 10 mA/cm^2 and at constant reaction time of 10 minutes and comparing it with a pure sample at the same conditions generated a similar oil and grease removal percentage with a slight edge for the pure sample over the different weights of the slag containing samples. Furthermore, it was seen that as the weight of the slag increases, the less the efficiency in the oil and grease removal is achieved. Moreover, the case for the TSS removal was the exact opposite where it was seen that a better TSS removal is achieved for the slag containing sample over the pure sample, and as the weight of the slag is increase the better the TSS removal is achieved. As for the turbidity, the effect of increasing the slag weight resulted in decreasing the removal effectively due to either the dust particle within the slag pore or the slag sticking to the magnetic stirrer, all while maintaining a high removal performance over the pure sample. The Variation of the pH of the solution and the conductivity were monitored during the reaction time and variation in their reading was reordered. However, these variations can be said to be random due to the complex nature of the chemical reaction taking place with the slag containing samples.

For any further work to be conducted with steel slag EC system, it is recommended to start with a current Density of 30 mA/cm^2 at a 30 minutes' reaction to obtained the optimum removal in terms of TSS, turbidity and oil and grease at a low power consumption.

REFERENCES

Adham, S. (August 2015). Desalination needs andopportunities in the oil & gas industry. Paper presented at the International Conference on Emerging Water Desalination Technologies in Municipal and Industrial Applications, San Diego, California, USA.

Argast, A., & F. Tennis III, C. (2007). A Web Resource for the Study of Alkali Feldspars and Perthitic Textures Using Light Microscopy, Scanning Electron Microscopy and Energy Dispersive X-ray Spectroscopy , *Journal of Geoscience Education 52(3),213-217.*

Arthur, J. D., Langhus, G. B., & Patel, C. (2005). Technical summary of oil & gas produced water treatment technologies. In. South Cheyenne Ave., Tulsa: ALL Consulting.

Bande, R. M., Prasad, B., Mishra, I. M., & Wasewar, K. L. (2008). Oil field effluent water treatment for safe disposal by electroflotation. *Chemical Engineering Journal, 137*(3), 503-509. doi:http://dx.doi.org/10.1016/j.cej.2007.05.003

Bennett, G. F., & Peters, R. W. (1988). The removal of oil from wastewater by air flotation: A review. *Critical Reviews in Environmental Control, 18*(3), 189-253. doi:10.1080/10643388809388348

Chen, G. (2004). Electrochemical technologies in wastewater treatment. *Separation and Purification Technology, 38*(1), 11-41. doi:http://dx.doi.org/10.1016/j.seppur.2003.10.006

Chen, J. P., Chang, S.-Y., & Hung, Y.-T. (2005). Electrolysis. In L. K. Wang, Y.-T. Hung, & N. K. Shammas (Eds.), *Physicochemical Treatment Processes* (pp. 359-378). Totowa, NJ: Humana Press.

Chen, X., Chen, G., & Yue, P. L. (2002). Novel Electrode System for Electroflotation of Wastewater. *Environmental Science & Technology, 36*(4), 778-783. doi:10.1021/es011003u

CHIN , D. A. (2006). *Water-quality engineering in Natural Systems*. United States of America: A JOHN WILEY & SONS, INC.

Chou, W.-L., Wang, C.-T., & Huang, K.-Y. (2009). Effect of operating parameters on indium (III) ion removal by iron electrocoagulation and evaluation of specific energy consumption. *Journal of Hazardous Materials, 167*(1–3), 467-474. doi:http://dx.doi.org/10.1016/j.jhazmat.2009.01.008

Daneshvar, N., Ashassi Sorkhabi, H., & Kasiri, M. B. (2004). Decolorization of dye solution containing Acid Red 14 by electrocoagulation with a comparative investigation of different electrode connections. *Journal of Hazardous Materials, 112*(1–2), 55-62. doi:http://dx.doi.org/10.1016/j.jhazmat.2004.03.021

Demirci, Y., C. Pekel, L., & Alpbaz, M. (2015). Investigation of Different Electrode Connections in Electrocoagulation of Textile Wastewater Treatment. *International Journal of electrochemical science, 10*(2685 - 2693).

Elazzouzi, M., Haboubi, K., & Elyoubi, M. S. (2017). Electrocoagulation flocculation as a low-cost process for pollutants removal from urban wastewater. *Chemical Engineering Research and Design, 117*, 614-626. doi:http://dx.doi.org/10.1016/j.cherd.2016.11.011

Fengxian , L., Shanping, L., Clienglu , Z., & Haixia , Z. (1995). Application of corrosive cell process in treatment of printing and dyeing wastewater. *Environmental Protection of Chemical Industry*(250014).

Ghernaout, D., Badis, A., Kellil, A., & Ghernaout, B. (2008). Application of electrocoagulation in Escherichia coli culture and two surface waters. *Desalination, 219*(1), 118-125. doi:http://dx.doi.org/10.1016/j.desal.2007.05.010

Ghernaout, D., & Ghernaout, B. (2011). On the controversial effect of sodium sulphate as supporting electrolyte on electrocoagulation process: A review. *Desalination and Water Treatment, 27*(1-3), 243-254. doi:10.5004/dwt.2011.1983

Ghernaout, D., Naceur, M. W., & Ghernaout, B. (2011). A review of electrocoagulation as a promising coagulation process for improved organic and inorganic matters removal by electrophoresis and electroflotation. *Desalination and Water Treatment, 28*(1-3), 287-320. doi:10.5004/dwt.2011.1493

Keeper, G. (Producer). (2013). Water Soluble Organics: Definitions & Removal Methods.

Lin, S. H., Shyu, C. T., & Sun, M. C. (1998). Saline wastewater treatment by electrochemical method. *Water Research, 32*(4), 1059-1066. doi:http://dx.doi.org/10.1016/S0043-1354(97)00327-8

Merma, A. G., & Mauricio Leonardo, T. (2008). *Electrocoagulation applied to aqueous medium containing oil.* The Pontifical Catholic University of Rio de Janeiro, Https://doi.org/10.17771/PUCRio.acad.12209.

Merzouk, B., Gourich, B., Sekki, A., Madani, K., & Chibane, M. (2009). Removal turbidity and separation of heavy metals using electrocoagulation–electroflotation technique: A case study. *Journal of Hazardous Materials, 164*(1), 215-222. doi:http://dx.doi.org/10.1016/j.jhazmat.2008.07.144

Mhatre, S., Vivacqua, V., Ghadiri, M., Abdullah, A. M., Al-Marri, M. J., Hassanpour, A., Kermani, B. Electrostatic phase separation: A review. *Chemical Engineering Research and Design, 96*, 177-195. doi:10.1016/j.cherd.2015.02.012

Mines, C. S. o. (2009). An Integrated Framework for Treatment and Management of Produced Water. In technical assessment of produced water treatment technologies.

Mollah, M. Y. A., Morkovsky, P., Gomes, J. A. G., Kesmez, M., Parga, J., & Cocke, D. L. (2004). Fundamentals, present and future perspectives of electrocoagulation. *Journal of Hazardous Materials, 114*(1–3), 199-210. doi:http://dx.doi.org/10.1016/j.jhazmat.2004.08.009

Mollah, M. Y. A., Schennach, R., Parga, J. R., & Cocke, D. L. (2001). Electrocoagulation (EC) — science and applications. *Journal of Hazardous Materials, 84*(1), 29-41. doi:http://dx.doi.org/10.1016/S0304-3894(01)00176-5

Moussa, D. T., El-Naas, M. H., Nasser, M., & Al-Marri, M. J. (2017). A comprehensive review of electrocoagulation for water treatment: Potentials and challenges. *Journal of Environmental Management, 186, Part 1*, 24-41. doi:http://dx.doi.org/10.1016/j.jenvman.2016.10.032

Nanseu-Njiki, C. P., Tchamango, S. R., Ngom, P. C., Darchen, A., & Ngameni, E. (2009). Mercury(II) removal from water by electrocoagulation using aluminium and iron electrodes. *Journal of Hazardous Materials, 168*(2–3), 1430-1436. doi:http://dx.doi.org/10.1016/j.jhazmat.2009.03.042

Ngamlerdpokin, K., Kumjadpai, S., Chatanon, P., Tungmanee, U., Chuenchuanchom, S., Jaruwat, P., Hunsom, M. (2011). Remediation of biodiesel wastewater by chemical- and electro-coagulation: A comparative study. *Journal of Environmental Management, 92*(10), 2454-2460. doi:http://dx.doi.org/10.1016/j.jenvman.2011.05.006

Norman, D. (2017). Oil and Gas Resources.

Petroleum, Q. (2015). Oil & Gas Field. , accessed through Qatar Petrolum website on the 29th of april 2017.

Phalakornkule, C., Worachai, W., & Satitayut, T. (2010). Characteristics of Suspended Solids Removal by Electrocoagulation *International Journal of Chemical, Molecular, Nuclear, Materials and Metallurgical Engineering, 4*(5).

Pintor, A. M. A., Vilar, V. J. P., Botelho, C. M. S., & Boaventura, R. A. R. (2016). Oil and grease removal from wastewaters: Sorption treatment as an alternative to state-of-the-art technologies. A critical review. *Chemical Engineering Journal, 297*, 229-255. doi:http://dx.doi.org/10.1016/j.cej.2016.03.121

Rahmalan, m. (2009). *Electrocoagulation for suspended solid removal in domestic wastewater treatment.* Universiti Teknologi Malaysia,

Rincón, G. J., & La Motta, E. J. (2014). Simultaneous removal of oil and grease, and heavy metals from artificial bilge water using electro-coagulation/flotation. *Journal of Environmental Management, 144*, 42-50. doi:http://dx.doi.org/10.1016/j.jenvman.2014.05.004

S. Blondes, M., Gans, K. D., L. Rowan, E., J. Thordsen, J., E. Reidy, M., A., . . . Thomas, B. (2016). *U.S. Geological Survey National Produced Waters Geochemical Database v2.2*. Retrieved from U.S. Geological Survey (USGS):

Systems, O. W. S. (2014). Pan America Environmental oil Water Separator operational Theory, Accessed on the 23rd of June ,2016 . Web address : http://www.oil-water-separator.net/separators-coalescing-theory.html

Terrazas, E., Vázquez, A., Briones, R., Lázaro, I., & Rodríguez, I. (2010). EC treatment for reuse of tissue paper wastewater: Aspects that affect energy consumption. *Journal of Hazardous Materials, 181*(1–3), 809-816. doi:http://dx.doi.org/10.1016/j.jhazmat.2010.05.086

Thella, K., Verma, B., Srivastava, V. C., & Srivastava, K. K. (2008). Electrocoagulation study for the removal of arsenic and chromium from aqueous solution. *Journal of Environmental Science and Health, Part A, 43*(5), 554-562. doi:10.1080/10934520701796630

Ting, T.-M., & Dahlan, K. Z. M. (2011). Electron beam decomposition of pollutant model compounds in aqueous systems. *Nukleonika, 56*(4).

Tir, M., & Moulai-Mostefa, N. (2008). Optimization of oil removal from oily wastewater by electrocoagulation using response surface method. *Journal of Hazardous Materials, 158*(1), 107-115. doi:http://dx.doi.org/10.1016/j.jhazmat.2008.01.051

Vepsäläinen, M. (2012). Electrocoagulation in the treatment of industrial waters and wastewaters. (Doctorate), Doria, Julkaisija – utgivare.

Volkov, A. G., Deamer, D. W., Tanelian, D. L., & Markin, V. S. (1996). Electrical double layers at the oil/water interface. *Progress in Surface Science, 53*(1), 1-134. doi:http://dx.doi.org/10.1016/S0079-6816(97)82876-6

Xu, P., Cath, T., & E. Drewes, J. ö. (2011). *Novel and Emerging Technologies for Produced Water Treatment.* Paper presented at the US EPA Technical Workshops for the Hydraulic Fracturing, Arlington, VA.

Xu, X., & Zhu, X. (2004). Treatment of refectory oily wastewater by electro-coagulation process. *Chemosphere, 56*(10), 889-894. doi:http://dx.doi.org/10.1016/j.chemosphere.2004.05.003

Öztürk, T., Veli, S., & Dimoglo, A. (2013). The Effect of Seawater Conductivity on the Treatment of Leachate by Electrocoagulation. *Chemical and biochemical engineering quarterly*, 27(3), 347-354. doi:http://hrcak.srce.hr/108955

Şengil, İ. A., & özacar, M. (2006). Treatment of dairy wastewaters by electrocoagulation using mild steel electrodes. *Journal of Hazardous Materials, 137*(2), 1197-1205. doi:http://dx.doi.org/10.1016/j.jhazmat.2006.04.009